NUREG/CR-3895

Investigation of Cold Leg Water Hammer in a PWR Due to the Admission of Emergency Core Cooling (ECC) During a Small Break LOCA

Prepared by A. B. Jackobek, P. Griffith

Massachusetts Institute of Technology

Prepared for
U.S. Nuclear Regulatory
Commission

GPO Printed copy price: $4.50

NUREG/CR-3895
R2

Investigation of Cold Leg Water Hammer in a PWR Due to the Admission of Emergency Core Cooling (ECC) During a Small Break LOCA

Manuscript Completed: January 1984
Date Published: September 1984

Prepared by
A. B. Jackobek, P. Griffith

Massachusetts Institute of Technology
Department of Mechanical Engineering
Cambridge, MA 02139

Prepared for
Division of Accident Evaluation
Office of Nuclear Regulatory Research
U.S. Nuclear Regulatory Commission
Washington, D.C. 20555
NRC FIN B7229

ABSTRACT

Experimental studies using a protoypical experimental flow model of a pressurized water reactor (PWR) demonstrate water hammer in the cold legs due to the admission of emergency core cooling (ECC). Such water hammer can occur in an actual PWR during reflood provided there exists a stratified flow of steam and water in the cold legs. The hydraulic conditions in an actual PWR making it susceptible to such water hammer are postulated in this report. Calculations, based on a published criterion for water hammer initiation, show that the amount of ECC administered by the high pressure safety injection (HPSI) system, is not great enough to produce liquid depths in the cold leg which can lead to slug formation and subsequent steam bubble collapse water hammer. However,a few water hammers can occur during ECC as the cold leg is being refilled.

A simple analysis developed in this report calculates the water hammer pressures possible under these postulated flow conditions. Potentially dangerous water hammer pressures are predicted during reflood at high system operating pressures characteristic of a small-break loss-of-coolant accident (SB-LOCA). Similar calculations done for the geometry of the experimental apparatus were compared to measurements taken during water hammer.

CONTENTS

	PAGE
ABSTRACT	iii
ACKNOWLEDGEMENTS	vii
LIST OF FIGURES	viii
NOMENCLATURE	x
1. INTRODUCTION	1
2. EXPERIMENTAL STUDIES	2
2.1 Description of Experimental Apparatus and Instrumentation	2
2.1.1 Core	2
2.1.2 Steam Generator	2
2.1.3 Hot/Cold Legs	6
2.1.4 ECCS	6
2.2 Experimental Procedure	6
2.3 Flow Model Test Results	7
2.3.1 Water Hammer During ECC	7
2.3.2 Water Hammer Peak Pressure Measurements	11
2.4 PWR Simulation Accuracy	11
3. ANALYSIS	14
3.1 Criterion for Water Hammer Initiation	14
3.1.1 Background of Analysis and Criterion	14
3.1.2 Simplified Analysis and Criterion	15
3.2 Calculation of the Peak Pressure Rise During Water Hammer	18
3.2.1 Flow Configuration	18
3.2.2 Dynamics of the Plug in the Cold Leg	18

Table of Contents (cont.) PAGE

3.2.3 Dynamics of the Water Column Issuing from the Downcomer..... 22
3.2.4. Peak Pressure Calculation..... 23

4. DISCUSSION OF RESULTS..... 24

4.1 Comparision of Calculated Water Hammer Initiation to Experimental Results..... 24
4.2 Water hammer Pressure Predictions and Measurements..... 27

5. EVALUATION OF WATER HAMMER IN A PWR DURING ECC INJECTION.. 31

5.1 System State..... 31
5.2 Determination of Stages of Reflood That Can Result in Water Hammer..... 33
5.3 Calculation of Peak Pressure Rise During PWR Water Hammer..... 35

6. CONCLUSIONS..... 47

REFERENCES..... 48

ACKNOWLEDGEMENTS

This report was prepared under contract with the U.S. Nuclear Regulatory Commission, Division of Nuclear Regulatory Research. Our supervisor is Dr. Jorem Hopenfeld.

LIST OF FIGURES

FIGURE NO.		PAGE
1	Experimental Flow Model	3
2	Mechanical Drawing of Experimental Flow Model	4
3	Photograph of Experimental Flow Model	5
4	System State in Flow Model During ECC Leading to Cold Leg Water Hammer	8
5	Test Map of Flow Model Experiments During ECC	9
6	Water Level in Downcomer vs. ECC Flow-rate During Flow Model Experiments	10
7	Steam Bubble Collapse Water Hammer Process in Experimental Flow Model During ECC	12
8	Measured Water hammer Pressures During ECC Tests in Experimental Flow Model	13
9	Idealized Stratified Flow in the Cold Leg During ECC Used to Determine the "Absolute Stability Limit"	16
10	Geometric Formulae for Stratified Flow of Steam and Water in a Circular Pipe	19
11	Algorithm to Calculate the "Absolute Stability Limit" of Water hammer Initiation	20
12	Test Conditions that Resulted in the Initiation of Water hammer During ECC	25
13	Calculated Critical ECC Flow Rate Necessary to Cause Water hammer During ECC Tests as a Function of Water Inventory in Cold Leg	26
14	Calculated Downcomer Water Level Rise in Experimental Model During ECC	28
15	Dynamics of Liquid Plug During Steam Bubble Collapse Water Hammer in Experimental Flow Model	29
16	Dynamics of Water Column From Core Vessel During Steam Bubble Collapse Water Hammer In Experimental Flow Model	30

LIST OF FIGURES (continued)

FIGURE NO.		PAGE
17	Comparison of Calculated Pressure Rise During Water Hammer to Measured Pressures	32
18	Postulated Steam Bubble Collapse Water Hammer During ECC in a PWR (B&W plant shown)	34
19	Comparison of the Critical ECC Flow Rate Necessary to Cause Water hammer During ECC in a Typical Plant vs. the HPSI System Output of a W Plant	36
20	HPSI Flow Rate Output of a W Plant	37
21	Approximate Cold Leg Water Depths During ECC Reflood For Which Water Hammer is Predicted in a PWR	38
22	Postulated Steam Bubble Collapse Water Hammer During ECC in a CE-80 System Used to Calculate the Resulting Pressures	39
23	Summary of Pressure Loss Coefficients of a Full Scale PWR	40
24	Typical Calculation of the Water Column and Water Plug Velocities During Steam Bubble Collapse Water hammer in a PWR	41
25	Typical Calculation of the Water Column and Water Plug Positions During Steam Bubble Collapse Water hammer in a PWR	42
26	Dynamics of Water Column as a Function of Initial Water Column Length Assumed	44
27	Effect of Geomertrical Pressure Losses and Plug Growth on Maximum Obtainable Velocity During Steam Bubble Collapse	45
28	Calculated Water hammer Pressures as a Result of Stream Bubble Collapse Water Hammer During ECC in a PWR	46

NOMENCLATURE

		UNITS
A	Cross Sectional Area of Liquid Plug (equal to A_p)	ft^2
A_l	Liquid Flow Area	ft^2
A_p	Cross Sectional Area of Cold Leg Pipe	ft^2
A_s	Steam Flow Area	ft^2
C	Speed of Sound in an Elastic pipe	ft/sec
C_p	Specific Heat of Liquid	BTU/lbm'F
D_o	Diameter of Cold Leg Pipe	ft
f	Pipe Friction Factor (0.02 assumed)	none
Fr	Froude Number	none
g	Gravitational Acceleration	ft/sec
g_c	Conversion Constant (32.174)	lbm-ft/lb-sec^2
h_{fg}	Heat of Vaporization	BTW/lbm
k_p	A_l/A_p	none
K_{t1}	Total Pressure Loss Coefficient For Liquid Plug due to Fittings, etc.	none
K_{t2}	Total Pressure Loss Coefficient For Water Column due to Fittings, etc.	none
L_s	Length of Liquid Plug	ft
m	Mass of Liquid Plug	lbm
$\dot{m}_c$	Mass Flow Rate of ECC	lbm/sec
$\dot{m}_s$	Mass Flow Rate of Steam	lbm/sec
N_{TD}	Taitel-Dukler Stratified-Slug Flow Transition Parameter	none
P	System Operating Pressure	psi
Q	Volumetric Flow Rate	ft^3/sec
R	Radius of Cold Leg	ft

NOMECLATURE (continued)

S_I	Interface Perimeter of Liquid and Vapor At a Cross Section	ft
t	time	sec
T_o	Temperature of ECC Flow	'F
T_{sat}	Saturation Temperature	'F
V_l	Liquid Velocity	ft/sec
V_c	Velocity of Liquid at Overfall	ft/sec
V_{pl}	Velocity of Liquid Plug In Cold Leg	ft/sec
V_{p2}	Velocity of Water Column From Downcomer	ft/sec
V_s	Steam Velocity	ft/sec
X_{pl}	Leading Edge Position of Liquid Plug	ft
X_{p2}	Leading Edge Position of Water Column	ft
Y	Liquid Depth in Cold Leg	ft
Y_c	Critical Depth	ft
α	Void Fraction	none
ρ_s	Steam Density	lbm/ft^3
ρ_l	Liquid Density	lbm/ft^3

1. INTRODUCTION

Since the Three Mile Island accident, much work has been performed to understand the thermal-hydraulic system behavior of a pressurized water reactor (PWR) in response to a small-break loss-of-coolant accident (SB-LOCA). Because of the unforeseen complexity of the two-phase flow in various components, large and costly system codes sometimes fall short of accurately predicting system transient response. Scaled experimental flow simulations such as the Full-Length Emergency Cooling Heat Transfer (FLECHT) and Separate-Effects and System-Effects Tests (SEASET) have been undertaken to enhance our understanding of this problem.

From all the efforts having been devoted to this problem many peculiar states leading to flow instabilities have postulated and/or demonstrated. In some of these peculiar states the way in which the entire system reacts is still not fully understood, nor have the consequences been fully evaluated.

One peculiar state which will inevitably lead to a flow instability of some magnitude is the injection of ECC into voided cold legs. Previous ECC experiments conducted during the 1970's were concerned with large break LOCAs and had the goal of insuring adaquate core coverage. Flow slugging was observed during such tests with the resulting pressure fluctuations considered to be within acceptable limits for plant safety. At the same time, only minor pressure fluctuations were observed in Semi-Scale and LOFT tests during ECC testing (1).

The consequences of admission of ECC into voided cold legs during a SB-LOCA are greater however. Typically, a SB-LOCA is characterized by a slow depressuriation rate so that high operating pressures can be maintained even though there is enough coolant loss to void the cold legs. In addition no air will enter through the break to diminish steam condensation rates. This combination of conditions can lead to potentially dangerous peak water hammer pressure which may jeopardize plant safety.

To compliment the FLECHT-SEASET experiments, a prototypical low pressure 1/15 scaled experimental flow model of a PWR was constructed and used to simulate the injection of ECC. The goal of the testing was to determine the type of flow instabilities possible and to understand the system effects which govern its occurance. The results of the ECC tests are presented in this report. These experiments demonstrated substantial water hammer pressures in the cold legs during ECC injection.

Also in this report, an analysis of steam bubble collapse water hammer initiation based on the work first done by Bjorge (2) is used to predict the coolant flow rates for which water hammer could be expected during model testing. These calculations are compared to the experimental operating conditions during which water hammer actually occured. Then, the possible hydraulic state of an actual PWR during a SB-LOCA making it susceptible to cold leg water hammer due to the injection of ECC is postulated. Calculations, based on the criterion for water hammer initiation, are performed to determine the stages of ECC and associated

cold leg liquid depths that such water hammer is likely to occur. An analytical model is then derived to predict the potential water hammer pressures during water slug impact accounting for the inertial and flow resistances imposed by the geometry which may lessen the peak pressures possible. Two sets of calculations are made. One set is for the range of operating pressures and the geometry of the flow model. The other set is for the operating conditions of an actual PWR. Calculations made for the model geometry are compared to peak pressure measurements made during water hammer. The relevance of these test results and calculations is discussed.

2. EXPERIMENTAL STUDIES

2.1 Description of Experimental Apparatus and Instrumentation

The apparatus is approximately a 1/15 scale experimental flow model of a 2-loop (4 cold leg) PWR which is designed to withstand operation up to 150 psig, but generally operates below 50 psig. A schematic diagram of the experimental apparatus is shown in Figure 1. The model is a simulation of a PWR which is operating under natural circulation cooling after suffering a SB-LOCA. The flow model includes the essential components of a PWR except for a pressurizer (since it only operates at low pressure) and circulatory coolant pumps (which are shut off under such accident conditions.) The components of the model are constructed of stainless steel, copper, and brass in order to minimize corrosion. The detailed mechanical design is shown in Figure 2, and photographs of the apparatus are presented in Figure 3. The following sections describe each of the model's components.

2.1.1 Core

The core is a 15.5 inch by 10 inch in diameter stainless steel tank with a downcomer annulus of 1 inch. Steam is generated in the core by eight 1690 watt electrical heaters, or is available through the use of an external supply of steam. For ECC injection testing since the heaters are of an inadequate capacity to maintain system pressure and temperature, it is necessary to use the external supply of steam. Core plenum pressure is measured and water level indicators monitor the water level in the inner vessel and downcomer. A drain in the bottom of the tank allows for the removal of water from the core so that quasi-steady state operation can be simulated during ECC.

2.1.2 Steam Generator

Each steam generator is a 12.5 inch by 7 inch in diameter stainless steel tank containing three 0.5 inch ID U-tubes that protrude from the top of the vessel to 3.5, 5.6, and 7.4 inch heights. Fittings were designed so that boiler glass could be installed in the bend of each U-tube for flow visualization. Sealing is accomplished in these fittings through the use of O-rings which have to be replaced periodically because of wear. A bleed valve at the top of each U-tube allows for the removal of noncondensible gas which would diminish the condensation rates and hamper natural circulation. There is an additional bleed valve in the exit plenum to which each cold leg is

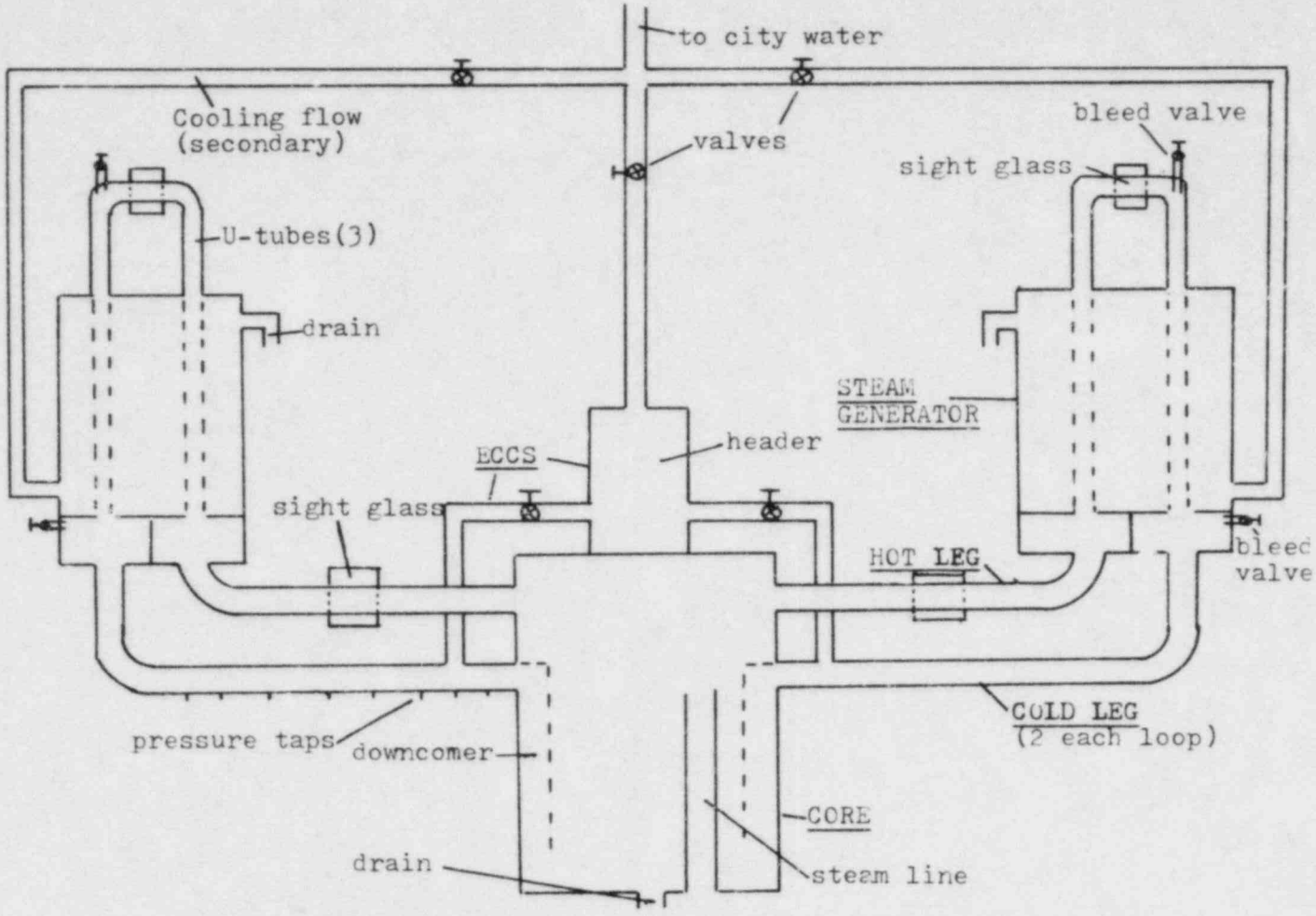

Figure 1 - EXPERIMENTAL FLOW MODEL

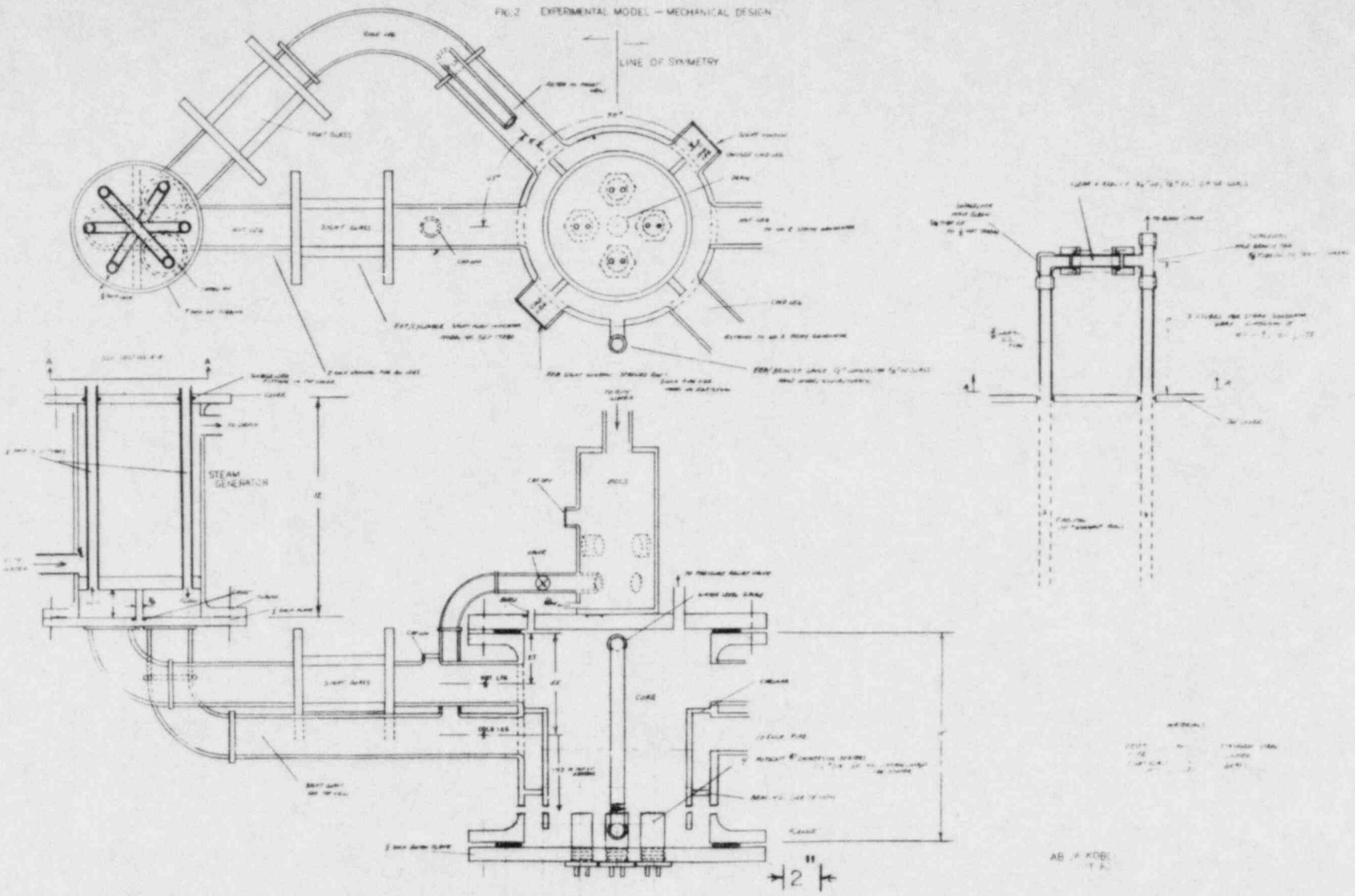

Figure 2 - Mechanical Drawing of Experimental Flow model

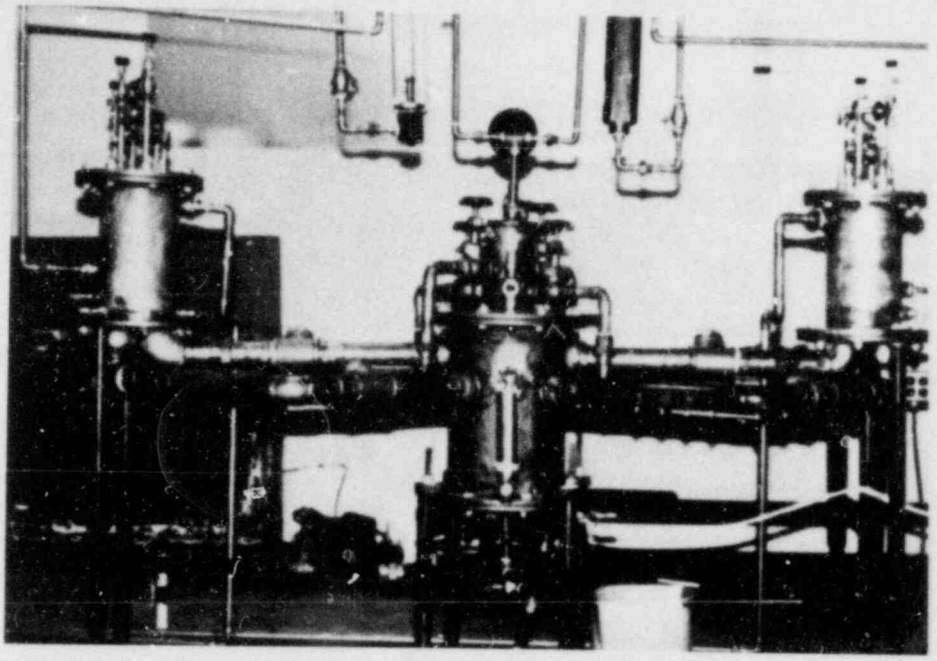

A. Front View

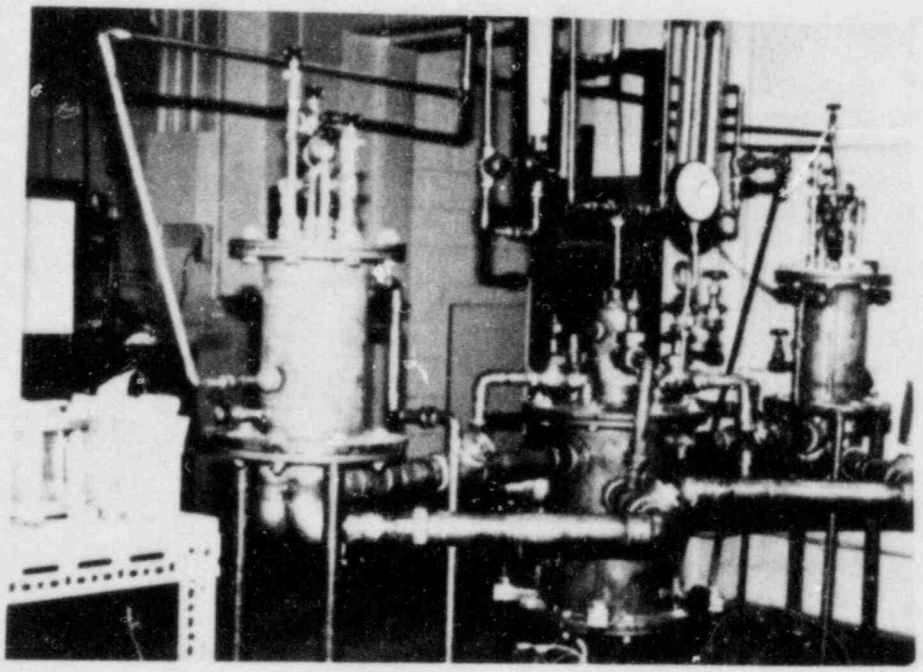

B. Side View

Figure 3 - Photographs of experimental flow model

attached. The U-tubes can be cooled by the cross flow of secondary coolant, entering near the bottom of the vessel and discharging at the top. A globe valve is used to adjust the amount of secondary coolant flow.

2.1.3 Hot/Cold Legs

Two steam generators are connected to the core by one hot and two cold legs made of standard 2 inch copper pipe. Flow visualization is made possible in each leg by the installation of a 2.5 inch ID by 5 inch sight glass or a sight window. Sight glasses or sight windows in the cold legs cannot be used during ECC injection tests because of excessive water hammer pressures. Pressure tap fittings made of 1/8 inch copper bushings were installed along the entire length of one of the cold legs to measure the peak pressure obtainable during water hammer. A high impedance pizoelectric pressure transducer, a Kisler model 566 charge amplifier, and a tektronics model 5111 storage oscilloscope were used to record the pressure transient during water hammer. The taps were installed in the bottom of the pipe to maintian a fairly constant temperature of the transducer so as to minimize thermal drift.

2.1.4 ECCS

The emergency-core-cooling system is simulated by the injection of coolant (water under city pressure) into each cold leg from a common header mounted on the top of the core vessel. The header is an 8.2 inch X 4.5 inch in diameter stainless steel tank. Flow is delivered from the common header to each cold leg by 1 inch copper tubing which is connected to each cold leg at a 90° angle. Valves in each line are used to adjust the flow rate. Additional fittings are included in the header to allow for the injection of coolant into the hot legs, however these were not used.

2.2 Experimental Procedure

The steam supply to the core is turned on and the system allowed to warm up so that all components are at their operating temperatures. Generally, a warm up time of 20 minutes is allowed for this. The secondary coolant flow is kept off so that steam may flow into the cold legs and not be condensed in the steam generators. The pressure in the core is then adjusted to below that of the ECC pressure by partially opening the core drain and throttling the steam supply valve. ECC flow is injected into the cold legs and measured by a rotometer. A desired core pressure and ECC flow rate are set and maintained by simultaneously adjusting ECC, steam, and core drain flow rates. All bleed valves are cracked open to remove noncondensibles that would decrease the steam condensing rate and hamper flow circulation.

Steam, driven by steam condensing in the coolant flow, is observed in the steam generator U-tube sight glasses to flow from the core through the hot legs and steam generators to the cold legs. Water levels in the core inner vessel and downcomer are noted.

The ECC flow rate is increased slightly, increasing the potential for a

greater steam flow, and the system is allowed to stabilize. If no flow instabilities are observed (e.g. water hammer), the ECC flow rate is again increased slightly and repeated until such an occurance. Once water hammer begins, the resulting pressures are measured at one of the pressure taps installed in the cold leg. This procedure is repeated for a variety of system operating pressures.

2.3 Flow Model Test Results

2.3.1 Water hammer During ECC

As the ECC system was activated, a natural circulation of steam developed that was driven by condensing steam in the cold legs. This flow configuration is depicted in Figure 4. In order to achieve this flow circulation, it was essential that the various bleed valves be opened to allow non-condensibles to escape from the system. In one particular test, the bleed valves were inadvertently left closed and the steam condensation rates were so low that there was no steam flow circulation at all. Despite these efforts to remove non-condensibles it is very likely that the system contained some amount of air, since the steam supply typically has an air volume fraction of 1 part in 10,000. This amount was not enough to impede circulation but could be enough to decrease the resulting water hammer pressures.

Once flow circulation was achieved, a stratified flow of steam and water existed in each cold leg, making the sytem susceptible to steam bubble collapse water hammer. To determine when water hammer could be triggered, a variety of system operating pressures and ECC flow rates were tested, as shown in Figure 5. Each test conducted is denoted by a particular symbol and the operating conditions for which water hammer was first observed are specified. No firm conclusions can be drawn from this graph, except that at high pressures water hammer occurred within a small range of ECC flow rates.

During all testing, the water inventory in the core inner vessel was maintained at a low and fairly constant level. The water level in the downcomer, however, uncontrollably rose above that in the inner vessel, behaving as a manometer to balance the pressure drop of the circulating steam. As the ECC injection flow was increased inducing a greater steam flow, the water level in the downcomer rose even higher. Water hammers were observed at approximately the same time as when the water level in the downcomer rose high enough to impede the free overfall of ECC into the core vessel. Figure 6 shows a plot of ECC flow rate vs. downcomer water level for two test runs during which there was a large difference in ECC flow rate prior to water hammer. As shown, water hammer occurred when the downcomer became full, and at no other time. Once the downcomer became filled to the level of the cold legs, the water depth in the cold legs would rise, decreasing the steam flow area. At a particular depth in the cold leg , a critical steam velocity leading to slug formation is achieved. This traps a steam bubble which collapses, resulting in water hammer.

Water hammers were heard in each of the cold legs throughout a test run and different components of the system would be rattled by the resultant

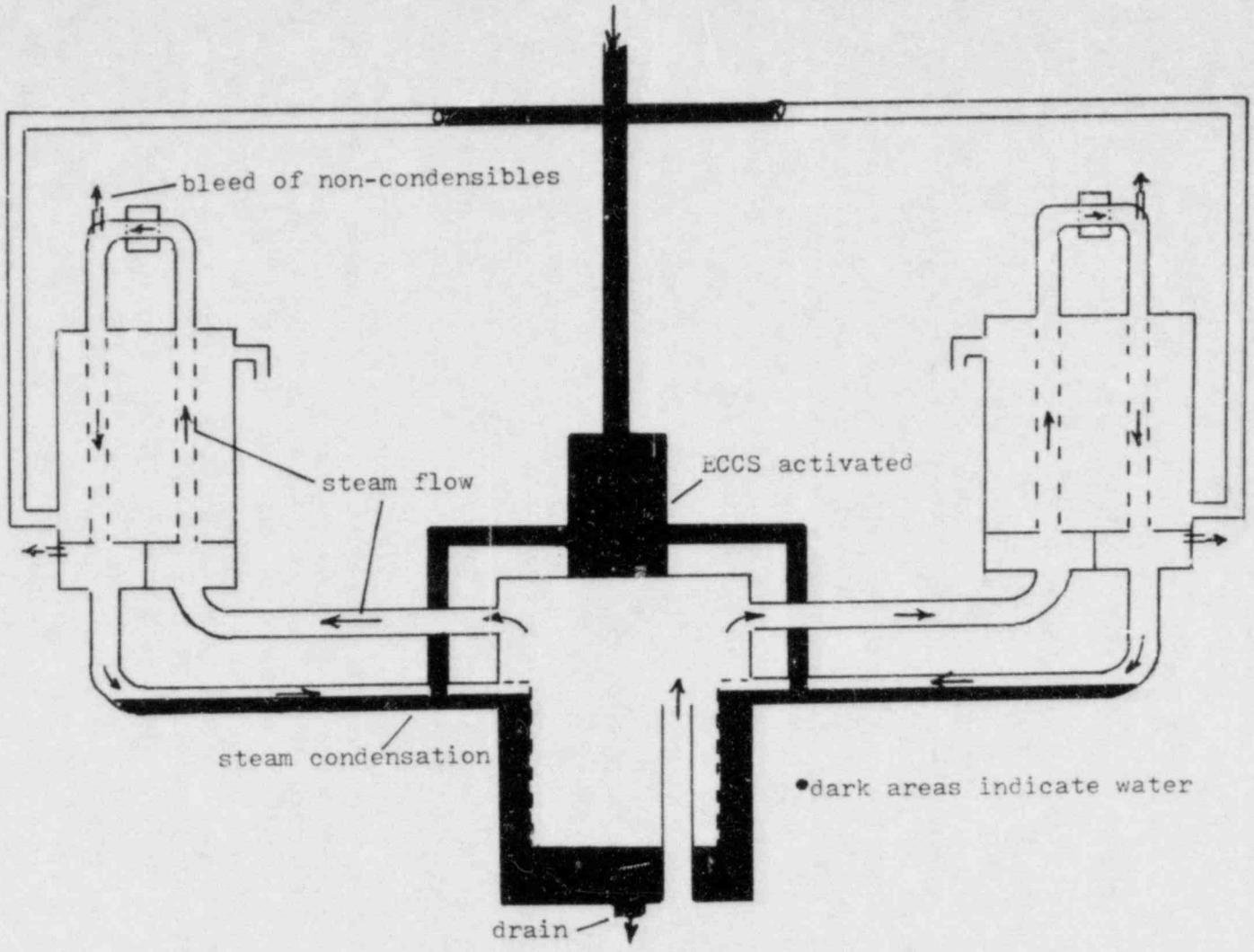

Figure 4 - System state in flow model during
ECC leading to cold leg water hammer

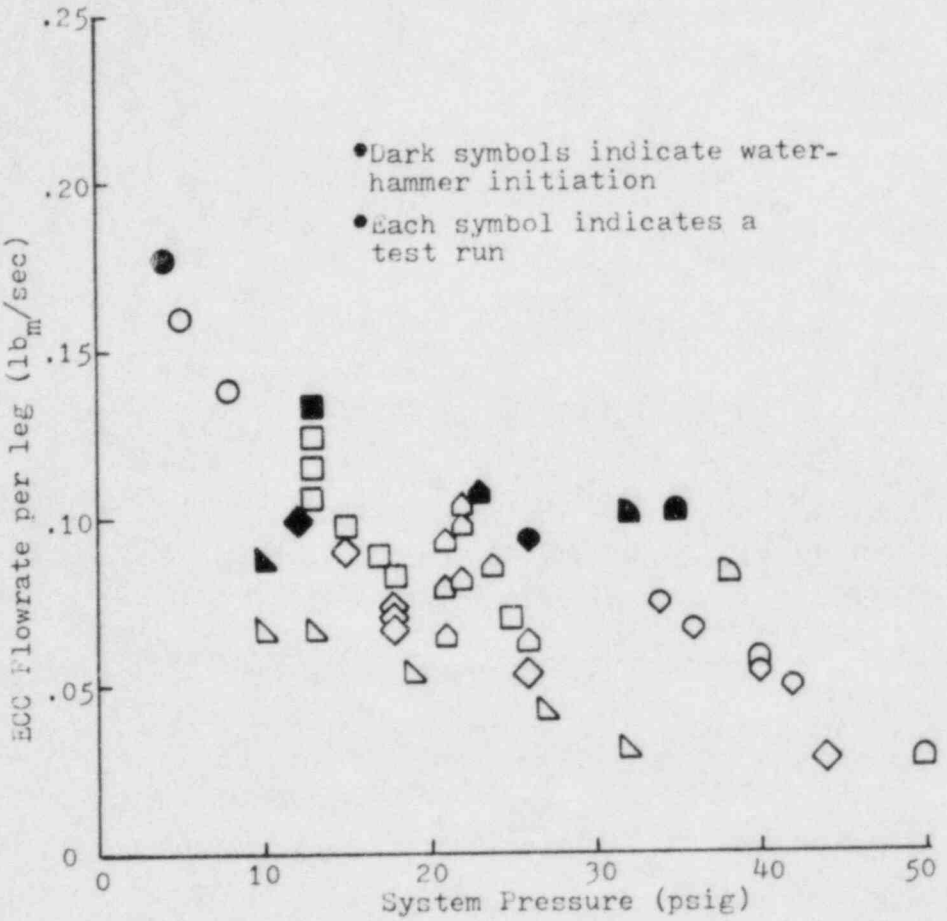

Figure 5 - Test map of flow model experiments during ECC

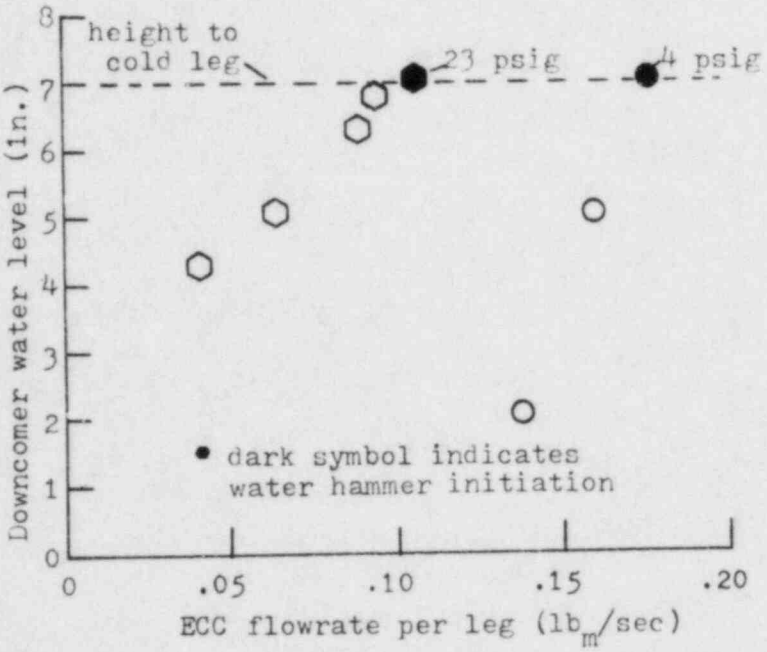

Figure 6 - Water level in downcomer vs. ECC flowrate during flow model experiments

pressures depending on the leg in which water hammer occured. However, it was very difficult to distinguish which of the four cold legs were hammering or to positively define any relationship between occurances in each of the legs. Though the water hammer occured in all legs, one was chosen fr the measurements because it appeared to be most prone to the hammers.

Once water hammer started, it could be maintained by draining water from the core and enabling the cold legs to remain somewhat voided. During successive water hammers, the water level in the core inner vessel fluctuated due to the continued entrainment of water into the cold legs during steam bubble collapse and expulsion of water after slug impact. The steam flow also varied, as observed in the sight glasses in each U-tube. When a water hammer occured in a particular cold leg, the resulting pressure wave would stall and reverse the steam flow in the corresponding steam generator. This happened momentarily until stratified flow conditions were reestablished in that cold leg. Steam would then proceed to flow in its original direction.

Since the flow was not visualized in each cold leg, the exact location of liquid slug formation was unknown. However, the most likely place for a slug to form is at the vicinity of discharge from the steam generator for the following reasons. The steam velocity is greatest here and the steam flow hits the water at an angle enhancing wave formation on the water interface, thus increasing the possibility of slug formation. Once the liquid slug forms, the steam bubble collapse process is presumed to occur as shown in Figure 7. The water plug and water column from the reactor vessel both having high pressure acting on one side, move rapidly into the void and then collide, producing a substantial pressure pulse.

2.3.2 Water hammer Peak Pressure Measurements

The pressure spikes produced during water hammer were measured along one of the cold legs in an attempt to measure at the point of slug impact and establish the severity of the water hammer pressures (See Figure 8). One cold leg was chosen for these measurements because it appeared to always produce water hammer throughout ECC injection testing. A more concentrated effort was devoted to obtain a large amount of data at those points where violent water hammer pressures occured most consistently. The pressure transducer was moved around in a search for the location at which the hammers were most frequent and violent. They were then left there. Locations where less frequent and milder water hammers occured were studied less diligently.

Generally, the greater the system operating pressure, the more violent the water hammer. Highest peak pressures were measured near the point of ECC injection suggesting slug impaction occured in this vicinity. The highest pressure measured was 1430 psi at the operating pressures of 30 and 40 psig.

2.4 PWR Simulation Accuracy

The experimental flow model does differ in some ways from an actual PWR

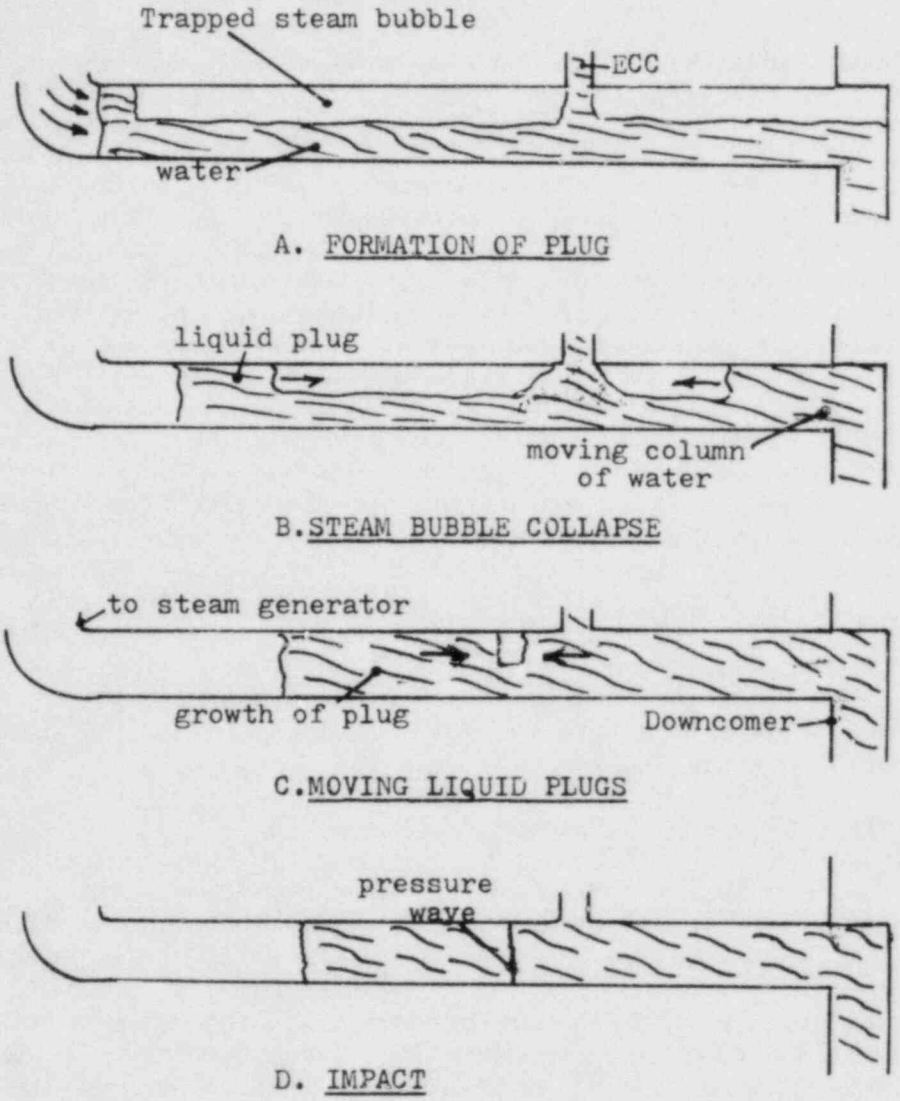

Figure 7 - Steam bubble collapse water hammer process in experimental flow model during ECC

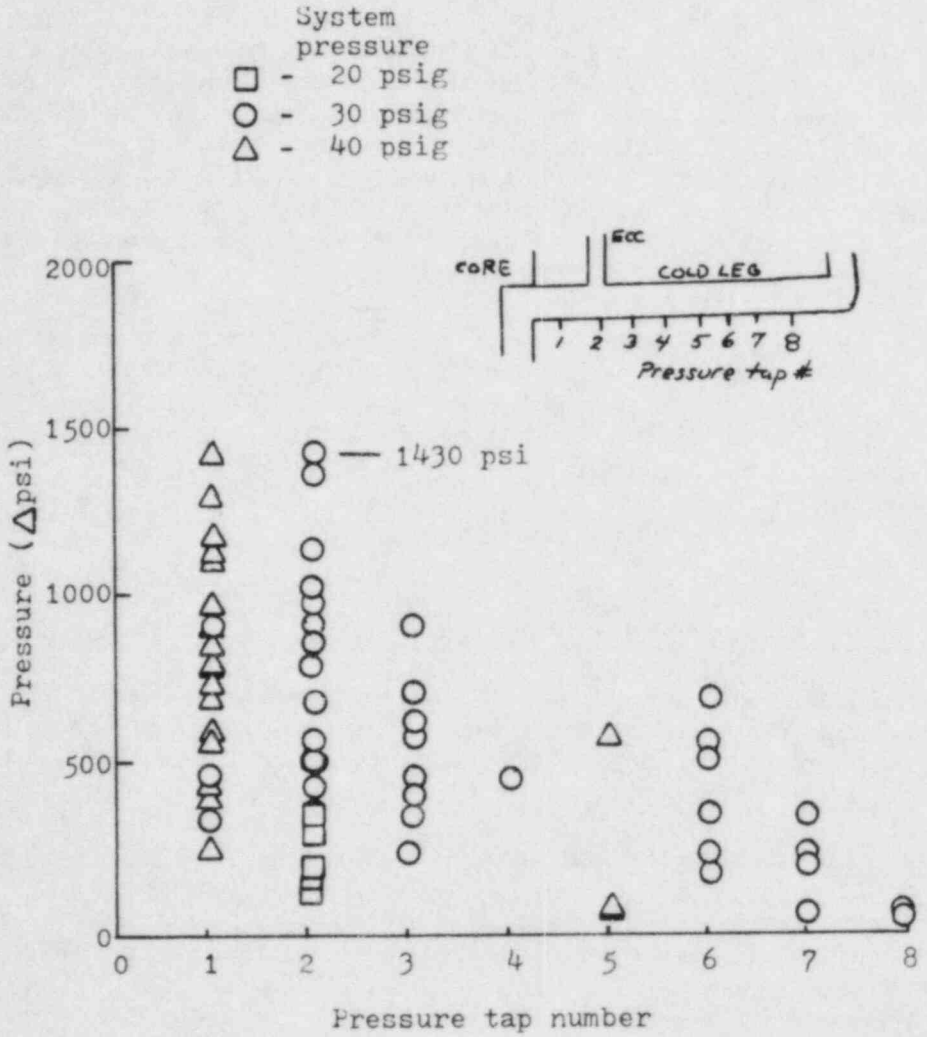

Figure 8 - Measured water hammer pressures during ECC tests in experimental flow model

which are relevant to the interpretation of the ECC injection testing. One dissimilarity is that the flow model does not have cold leg loop seals which may all become plugged during a SB-LOCA. If plugged, there would be no direct flow path for steam from the steam generator, as observed in these experiments. However, the loop seals need not all be plugged depending upon the events of the accident. There are also alternate steam flow paths which can result in a stratified flow of steam and water in the cold legs. For example, in a B & W reactor, a steam flow path can be available directly from the core through the vent valves. This bypass is present because the hot leg is not welded to the core-barrel assembly. To make repairs to the internals of the core-barrel assembly, the capability must exist to lift the assembly out of the vessel. Thus, the hot leg fits snugly against the core-barrel assembly but a bypass flow passes directly from the downcomer to the upper plenum during steady-state operation (3).

ECC was injected into the cold legs at a 90^{o} angle rather than at 60^{o} as it exists in the actual system. This changes the local liquid depth in the cold leg near the injection point and some of the intricacies of the steam water interface. However, as long as the coolant is being injected from above the cold leg, prototypical steam condensation rates are achieved.

3. ANALYSIS

3.1 Criterion for Water hammer Initiation

An analytical model was developed and used to predict critical ECC flow rates that could result in water hammer. This model was used to compare with model test results and to predict possible occurance in an actual PWR.

3.1.1 Background of Analysis and Criterion

Bjorge (2) developed a one dimensional flow model to describe the initiating mechanism associated with steam bubble collapse water hammer in a pipe containing steam and subcooled water. Using the stability criterion proposed by Taitel and Dukler (4) for the transition from stratified to slug flow, he was able to predict and verify experimentally the water flow rates which would cause water hammer. His analytical model first solved numerically for the one dimensional flow conditions in a pipe containing subcooled water and condensing steam. Then, by calculating the Taitel-Dukler criterion along the length of the pipe, the possibility of slug formation and subsequent water hammer could be determined. The "metastable limit" of water hammer initiation was defined as the minimum water flow rate necessary to satisfy the criterion at any position in the pipe.

Also defined in his thesis was an "absolute stability limit" which is a more conservative prediction of water hammer formation. This stability limit is defined as the minimum liquid flow rate necessary to satisfy the Taitel-Dukler criterion, assuming that the subcooled liquid entering a pipe is immediately heated to saturation temperature by the amount of steam flow necessary to accomplish this. Thus, a constant steam flow

rate and saturated liquid temperature are assumed at all cross sections along the length of the horizontal pipe.

3.1.2 Simplified Analysis and Criterion

The analytical model developed in this study follows the "conservative approach" and the equations developed basically follow the methodology developed by Bjorge, with some simplified assumptions. A stratified flow of steam and water exists in the cold leg as a result of ECC injection, as shown in Figure 9. The mass flow rate of steam is considered to be an amount necessary to achieve thermal equilibrium, e.g. complete mixing:

$$\dot{m}_s = \frac{m_c c_p (T_s - T_o)}{h_{fg}} \qquad (3\text{-}1)$$

It should be recognized that this steam flow rate is an upper limit. In general, some subcooling remains in the water and the steam flow rate is less. The water level in the cold leg is controlled by the free overfall of water ($m_c + m_s$) into the downcomer. If the water level in the downcomer reaches the height of the cold legs, then this will govern the water level in the cold leg. When free overfall conditions exist, then the liquid depth and flow rate in the pipe are related by the requirement that the specific energy of the fluid (that is the kinetic, plus potential energy) is at a minimum at the overfall and the Froude number is equal to 1. That is $(1/2/gD) = 1$. For a circular pipe, Chow (5) gives a relationship developed by Braine (6) in English Units for critical depth as a function of volumetric flow rate.

Eq. 3-2 is the critical depth for a Froude number of 1 evaluated for a circular pipe.

$$Y_c = 0.325 \, (Q/D_o)^{2/3} + 0.083 \, D_o \qquad (3\text{-}2)$$

Eq. 3-2 is appropriate as long as the dimensionless depth lies between:

$$0.3 \quad Y_c/D_o \quad 0.9 \qquad (3\text{-}3)$$

For the case of horizontal pipe flow, using the methods customary for open channel flows (5) one assumes an energy coefficient equal to 1. Since the specific energy of the fluid is at a minimum at the overfall, the velocity at the overfall is given by:

$$V_c^2 = Y_c g \qquad (3\text{-}4)$$

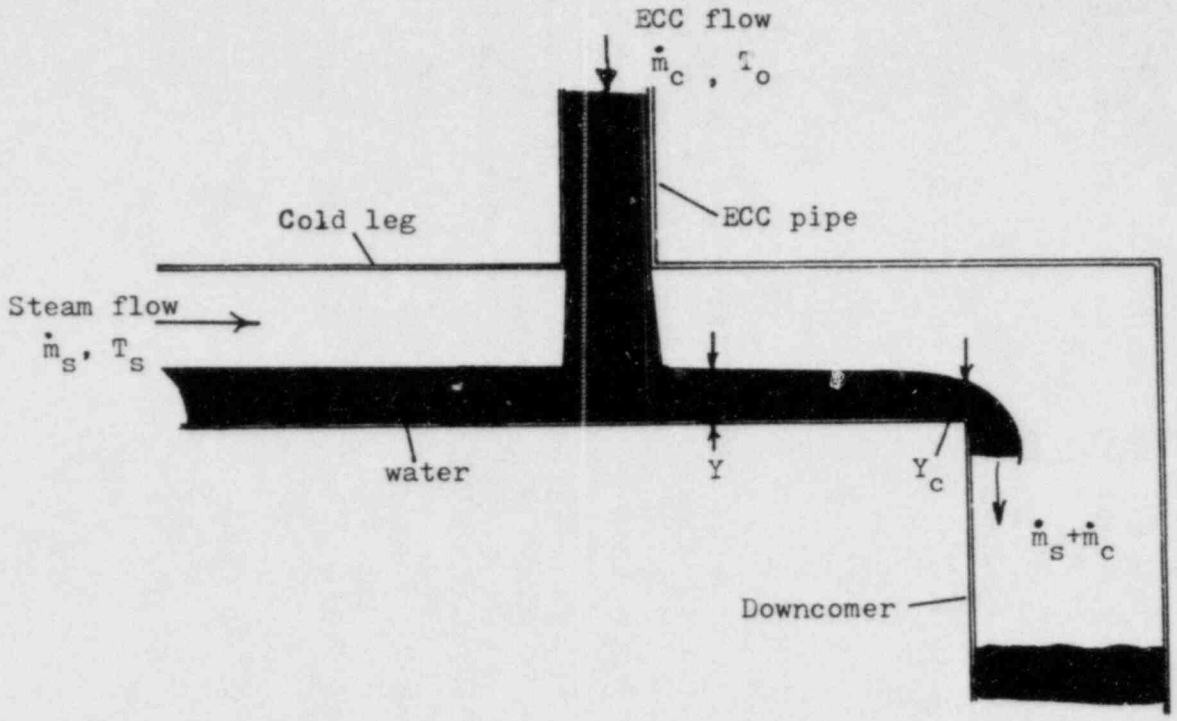

Figure 9 - Idealized stratified flow in the cold leg during ECC used to determine the "absolute stability limit"

The specific energy is thus the sum of kinetic plus potential energy or

$$E = \frac{3}{2} Y_c \quad \bullet \tag{3-5}$$

Neglecting frictional losses in the pipe, the total energy remains constant throughout the pipe and thus at the ECC injection point:

$$Y + V_1^2/(2g) = \frac{3}{2} Y_c \tag{3-6}$$

$V_1^2/2g$ is generally small compared to Y, thus the maximum liquid depth in the pipe is given by:

$$Y = \frac{3}{2} Y_c \tag{3-7}$$

This is a well known result for open channel flows and appears in most texts on the subject.

As previously discussed, water hammer is initiated when the flow regime changes from stratified to slug flow and the Taitel-Dukler criterion can be used to predict this occurance. Flow transition is predicted when the Taitel-Dukler number is at least equal to unity where:

$$N_{TD} = \frac{1-\alpha}{\alpha} \frac{\rho_s}{\rho_1} \frac{V_s^2}{V_1^2} \frac{Fr}{(1-Y/D_o)^2} \tag{3-8}$$

Eq. 3-8 can also be expressed as:

$$N_{TD} = \frac{1-\alpha}{\alpha} \frac{\rho_s}{\rho_1} \frac{S_I}{g} \frac{V_s^2}{A_1 (1-Y/D_o)^2} \tag{3-9}$$

Figure 10 shows formulae used to calculate the necessary geometric parameters and the velocity of steam is given by:

$$V_s = \frac{\dot{m}_s}{\rho_s A_s} \qquad (3\text{-}10)$$

For a given ECC flow rate, Eq. 3-1 is used to calculate the steam mass flow rate, Eq. 3-2 and 3-7 used to calculate the critical depth and liquid depth in the pipe respectively, and with the necessary geometric calculations, Eq. 3-9 used to determine if water hammer will occur.

A computer program was written to implement the equations and iterate on the critical ECC flow rate necessary to make the Taitel-Dukler number (N_{TD}) just equal to unity, the onset of water hammer. Figure 11 shows the algorithm used in this program.

3.2 Calculation of the Peak Pressure Rise During Water Hammer

A simplified analysis was used to calculate the magnitude of the pressure spike as a result of cold leg water hammer during ECC in a PWR and in the model geometry to use for comparison with the peak pressure measurements made during water hammer. Previous work has been done on steam bubble collapse water hammer, and pressure measurements have been conducted under much more controlled experimentation (7). The model developed here is not intended to duplicate or improve any work that has already been done, but rather to define a simple model that describes the likely flow configuration during steam bubble collapse accounting for the mechansims which have a calculable effect on the peak pressure obtainable during water hammer.

3.2.1 Flow Configuration

The scenario of events leading to water hammer during ECC cold leg injection in the model geometry have been discussed in Section 2. As previously stated, a likely place for a slug to form in the flow model geometry is at the vicinity of discharge from the steam generator. This traps an amount of steam of length approximately equal to the length of the cold leg. When the steam bubble collapses, the water plug and water from the reactor vessel move rapidly into the void and collide, resulting in an impact pressure pulse. Figure 7 depicts this series of events.

3.2.2 Dynamics of the Plug in the Cold Leg

To obtain the impact velocity, the dynamics of the water plug that forms in the cold leg are calculated by applying Newton's Second Law of Motion. On this basis, the following simplifying assumptions are made:

a) System pressure acts on one side of the liquid plug and zero pressure exists inside the steam bubble upon collapse. (The

Pipe less than half full

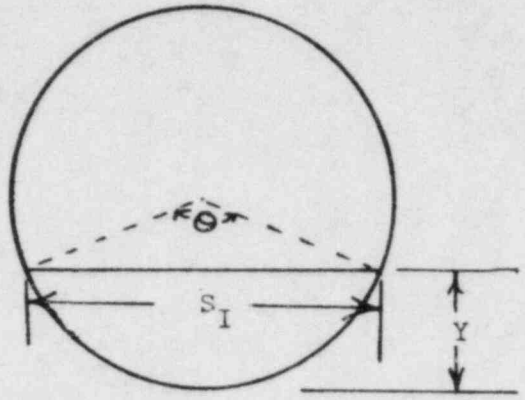

$$S_I = 2(Y(D-Y))^{1/2}$$

$$\Theta = 2\tan^{-1}\left[\frac{S_I/D}{(1-(S_I/D)^2)^{1/2}}\right]$$

$$A_1 = (\Theta - \sin\Theta)D^2/8$$

Pipe greater than half full

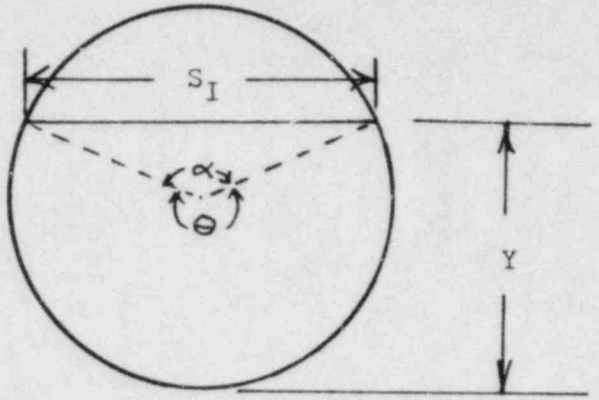

$$S_I = 2(Y(D-Y))^{1/2}$$

$$\alpha = 2\tan^{-1}\left[\frac{S_I/D}{(1-(S_I/D)^2)^{1/2}}\right]$$

$$\Theta = 2\pi - \alpha$$

$$A_1 = (\Theta - \sin\Theta)D^2/8$$

For pipe half full :

$$A_1 = \pi D^2/8$$

Figure 10 - Geometric formulae for stratified flow of steam and water in a circular pipe

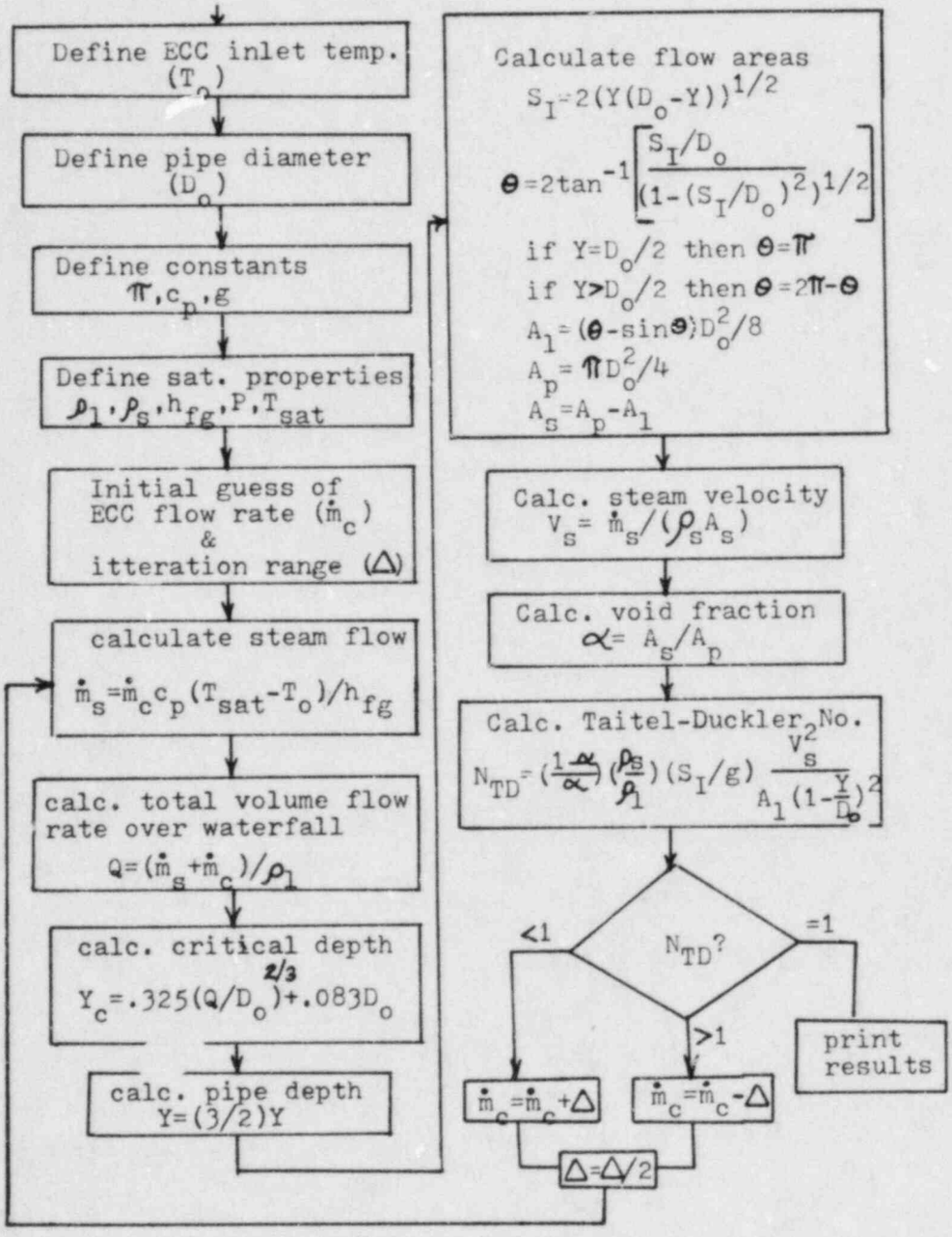

Figure 11 - Algorithm to calculate the "absolute stability limit" of water hammer initiation

non-condensible gas pressure is essentially zero if a water hammer is to occur because if it were significant the condensation rate would be very much reduced. Similarly, the saturation pressure at the temperature of the ECC is negligible compared to the system pressure.)

b) The mass of the liquid plug increases as it accelerates through the void by entraining the water that is below the void.

c) The motion of the plug is retarded by pipe friction and momentum loss mechanisms. For reasons, which we still don't understand, condensation is an exceedingly rapid process so that almost a step reduction in pressure occurs when the condensation event is indiated.

Accounting for the change in the mass of the plug as a function of time assuming the added mass is initially at rest, Newton's Second Law for a control volume traveling with the plug, becomes

$$\Sigma F_x = \frac{\partial}{\partial t} \int_o^L \rho V_x A dx + \int_{A_{out}} \rho V_x^2 dA - \int_{A_{in}} \rho V_x^2 dA \qquad (3\text{-}11)$$

and the resulting differential equations of motion are as follows.

$$\frac{d V_{pl}}{dt} = \frac{PAg_c}{m} - \frac{\rho_l V_{pl}^2 A}{m} (K_p+1) - \frac{f \rho_l V_{pl}^2}{8 m} \pi D_o L_s - K_{tl} \frac{\rho_l V_{pl}^2 A}{2 m} \qquad (3\text{-}12)$$

To obtain Eq. 3-12 from Eq. 3-11 one evaluates the pressure drops from the fittings in the pipe and adds to this the pressure difference evaluated from the momentum equation. One then solves the resulting equation for (dV_{pl}/dt) and divides through by (m/g_c).

Eq. 3-13 below is the continuity equation and relates the advance rate of the front of the slug to the velocity of the slug. Eqs. 3-14 and 3-15 are geometric conditions.

$$\frac{d x_{pl}}{dt} = (1 + K_p) V_{pl} \qquad (3\text{-}13)$$

$$\frac{dm}{dt} = \rho_l V_{pi} K_p A \qquad (3\text{-}14)$$

$$\frac{dL_s}{dt} = K_p V_{pl} \qquad (3\text{-}15)$$

The rate of mass increase of the liquid plug is accounted for by adjusting the size of the liquid plug by the amount of liquid the plug sweeps up as it travels through the void (Kp is the portion of the pipe area which is water). In the absence of assumptions (b) and (c) Eq. 3-11 reduces to the calculation of the velocity of the plug based on conservation of energy (so that the final kinetic energy is equal to the PV work doen by the condensing bubble. That is

$$V_{pl} = \left[\frac{2 P_{gc} X_{pl} (1-K_p)}{\rho_\ell L_s} \right]^{\frac{1}{2}} \qquad (3\text{-}16)$$

where X_{pi} is equal to the length of the trapped steam bubble.

Eq. 3-12 shows that the maximum obtainable velocity is limited by the liquid plug growth and frictional/momentum change losses. For any calculation, an inital plug length must be known or assumed and is important in determining the time it takes for the plug to reach its maximum or terminal velocity. When substantial flow resistances are present in the system the impact velocity and thus the calculated pressure spike are not sensitive to the initial plug size as long as impact occurs when the plug has obtained a terminal velocity since this velocity is limited by the factors previously mentioned. The differential equations of motion, being non-linear, are solved numerically by Runga-Kutta to determine the leading edge position and velocity of the plug as a function of time.

3.2.3 Dynamics of the Water Column Issuing from the Downcomer

The water column that flows from the core's downcomer during steam bubble collapse is idealized as shown in Figure 7. The static pressure at the downcomer exit acting on the water column is calculated from Bernoulli's equation accounting for exit loss effects. Then, making the rest of the same assumptions as in Section 2, the following equations

are obtained:

$$\frac{dV_{p2}}{dt} = \frac{Pg_c}{\rho_1 x_{p2}} - (1+K_{t2}+2K_p)\frac{V_{p2}^2}{2x_{p2}} - \frac{f\,V_{p2}^2}{2D_o} \qquad (3\text{-}17)$$

$$\frac{dx_{p2}}{dt} = (1+K_p)\quad V_{p2} \qquad (3\text{-}18)$$

Assuming the flow is originating from a plenum, an effective additional water column length was assumed. This is equal to a column length of $D_o/4$. This accounts for the additional kinetic energy the liquid in the vicinity of the cold leg discharge into the down commer. That is

$$\text{Effective Water Column Length} = \frac{D_o}{4} \qquad (3\text{-}19)$$

As will be shown, the terminal velocity is not very sensitive to the choice of effective column length. These equations are again solved numerically.

3.2.4 Peak Pressure Calculation

A Conservative calculation for the water hammer peak pressure asumes the plug velocities are extinguished upon impact. The pressure rise is then calculated by:

$$\Delta P = \frac{\rho_1\,(V_{p1}+V_{p2})\quad C}{g_c} \qquad (3\text{-}20)$$

The impact velocities V_1 and V_2 of each liquid plug are determined by solving the plug dynamic equations as outlined in sections 2 and 3. The impact velocity is determined at the time which both plugs enguif the entrapped steam bubble.

Neglecting wall friction and momentum changes as compared to the various pipe flow resistances due to berds, area changes, water level in the pipe, etc... which are generally much greater, the obtainable velocities of the liquid plug and water column as calculated from Eq. 3-12 and 3-17 are as follows. (It is assumed, as before, that P bubble =0).

$$V_{p1}^2 = \frac{1}{K_{t1}+2K_p}\,\frac{2g_cP}{\rho_1} \qquad (3\text{-}21)$$

$$V_{p2}^2 = \frac{1}{1+K_{t2}+2K_p} \frac{2g_c P}{\rho_1} \qquad (3\text{-}21)$$

The difference between these two equations arises because of the difference in the assumed static pressure acting on the plug versus the water column. In essence the two water slugs are accelerated up to the velocity at which the pressure loss in the fittings equals the driving pressure for each plug. These equations can be used to calculate the potential impact velocities. They provide consistant answers with calculations made by solving the differential equations when the liquid plug and column are restricted by the factors mentioned and the trapped steam bubble is sufficient in length as compared to the initial plug size as can be ascertained by Eq. 3.16.

4. DISCUSSION OF RESULTS

4.1 Comparision of Calculated Water Hammer Initiation to Experimental Results

Figure 12 shows those test conditions for which water hammer was observed. As discussed prviously, water hammers always occurred at ECC injection flow rates when the water level in the core vessel downcomer rose high enough to prevent a free overfall of coolant into the downcomer annulus. This level controlled the liquid depth in the cold leg. Therefore, the critical steam velocity necessary to initiate water hammer was acheived at a lower ECC injection flow rate (or lower steam flow rate) than if free fall conditions had prevailed at exit from the cold leg.

Figure 13 is a calculation of the ECC flow rate expected to result in water hammer depending on the water level in the cold leg using the flow transition criterion of Taitel and Dukler as discussed in Section III and assuming thermal equilibrium. Typically, the ECC water temperature was in the range of $80^{\circ}F$ - $120^{\circ}F$ depending on the extraneous sources of heating in the laboratory, so an average ECC temperature of $100^{\circ}F$ was used for this calculation.

Based on the typical ECC flow rates for which water hammers were observed, this calculation implies that the cold leg was appoximately half full when water hammer occured. Although the exact water level in the cold leg was not measured during water hammer, the water level gauge in the downcomer did extend to approximately the center line of the cold leg and was completely filled prior to water hammer formation. Therefore, this calculation is consistant and fairly reasonable. The actual water depths would have to be at least that given by Figure 13 and most likely somewhat higher depending on how close the actual steam flow is to the amount necessary to achieve thermal equilibrium.

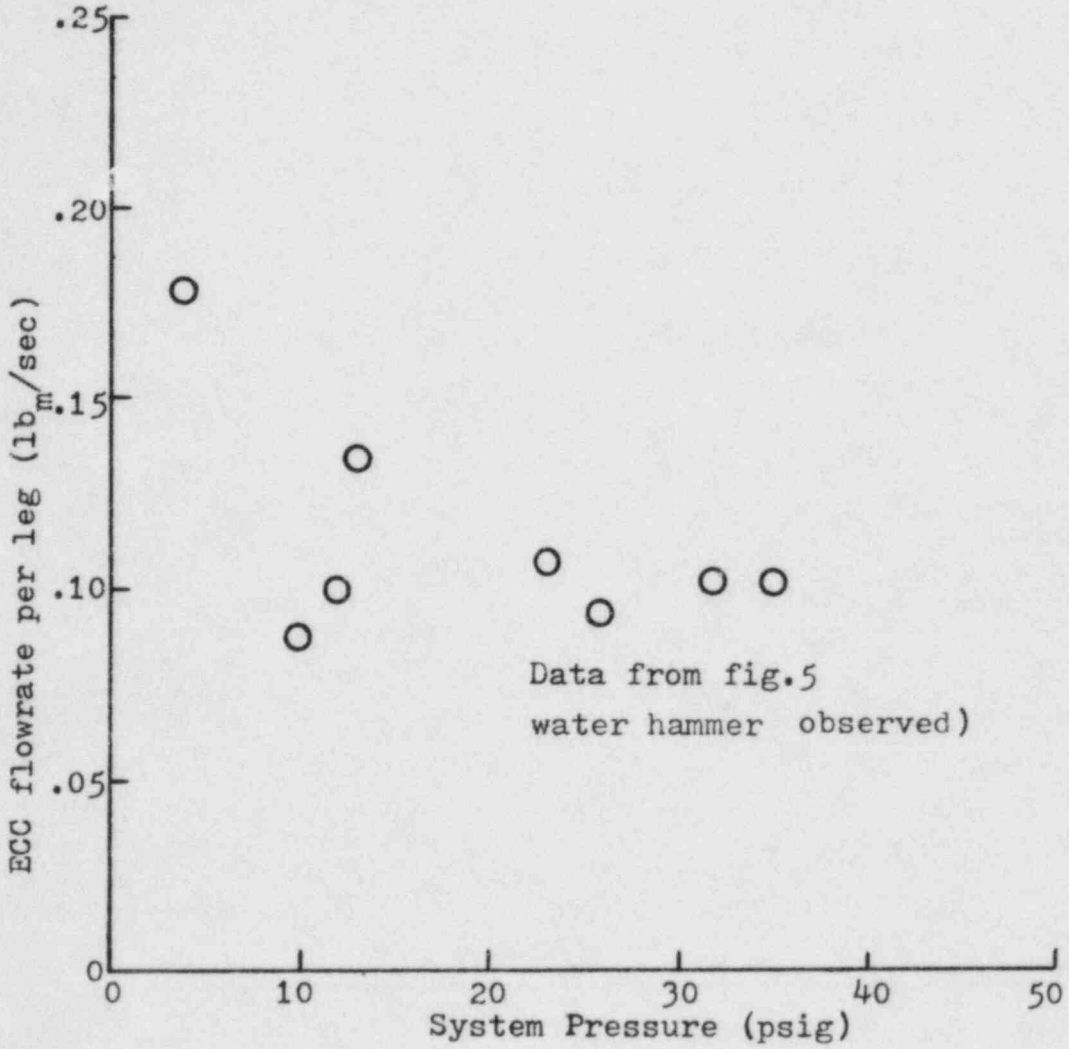

Figure 12 - Test conditions that resulted in the initiation of water hammer during ECC

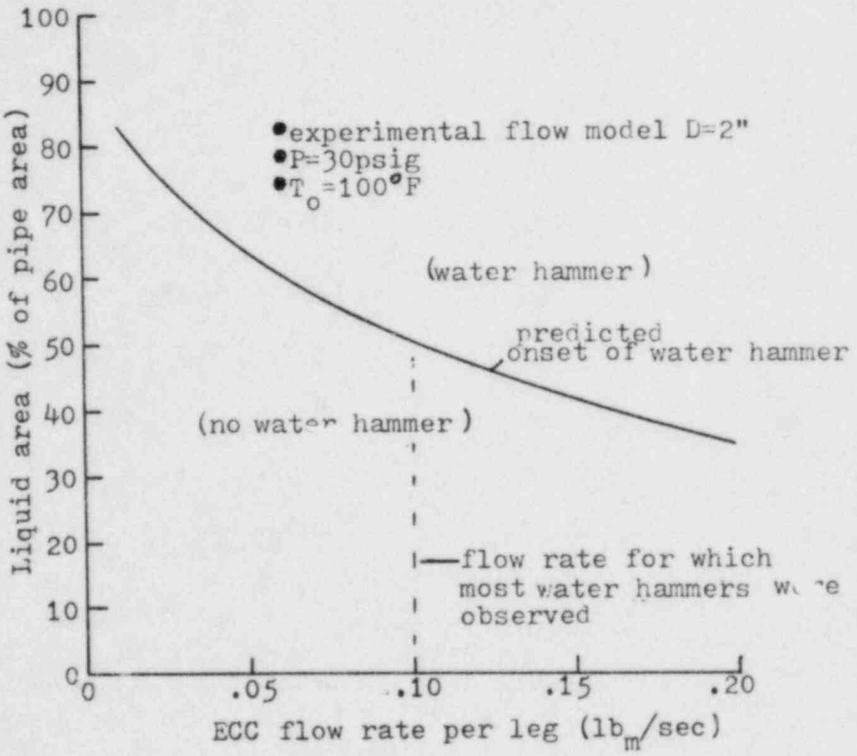

Figure 13 - Calculated critical ECC flow rate necessary to cause water hammer during ECC tests as a function of water inventory in cold leg

The pressure drop of the circulating steam was calculated in order to provide an explanation for the degree of water level rise in the downcomer during the admission of ECC. Figure 14 shows the calculated pressure drop as a function of the ECC injection flow rate and amount of subcooling assuming condensation rates necessary to achieve thermal equilibrium. These results do explain the hydraulic flow conditions observed. The pressure drop as calculated can be great enough to cause the water level in the downcomer to rise to the height of the cold legs (approximately 7 inches). The major portions of this pressure drop are primarily the pressure drop through the three 1/2 inch ID steam generator U-tubes and secondarily, the pressure drop through the cold leg as the water depth increases. The calculated pressure drop, however, is somewhat greater than that measured by the water level rise in the core downcomer. This in all likelyhood is due to achieving steam flow rates less than that amount assuming thermal equilibrium. In any event, the trends observed during experimentation are consistent with this analysis. In fact, the ECC flow rate for which the water level in the core downcomer rose high enough to block the free overfall of coolant into the core and that predicted to produce such a circulating steam pressure drop are lower than the ECC flow rate necessary to produce liquid depths to cause water hammer with a free overfall boundary condition. For example at a system operating pressure of 30 psig and ECC coolant temperature of 100°F, the ECC flowrate would have to be at least 0.21 lbm/sec per leg in order to cause such "Bjorge-type" water hammer.

In summary, the model test results show that water hammers can occur during cold leg ECC injection as the water level in the cold leg becomes high enough, resulting in the formation of a liquid plug that traps a steam bubble. This occurred during experimental testing when the water level rise in the core vesel downcomer that balanced the circulating steam pressure drop governed the water level in the cold leg. The experimental flow model geometry is such that this phenomenum occurred prior to acheiving ECC flow rates that could also lead to water hammer formation as predictable from the analysis of Bjorge.

4.2 Water Hammer Pressure Predictions and Measurements

The equations described in Section 3, using the pressure loss coefficients applicable to the geometry were solved numerically. Figures 15 and 16 are the result of a typical calculation for an operating pressure of 40 psig which shows the position and velocity as a function of time for the liquid plug assumed to be formed in the cold leg and the column of water expected to be entrained from the core vessel downcomer. The water level in the cold leg during water hammer was unknown so a liquid depth of 1/2 the diameter based on Figure 13 was used.

The impact velocities of the plugs are determined when the sum of the leading edge position traveled by both plugs is equal to the length of the trapped steam bubble (in this case, the entire length of the cold leg). Based in the initial plug lengths assumed, the liquid plug transients are very short in duration and therefore, the impact velocities are calculated to be the terminal or maximum obtainable plug

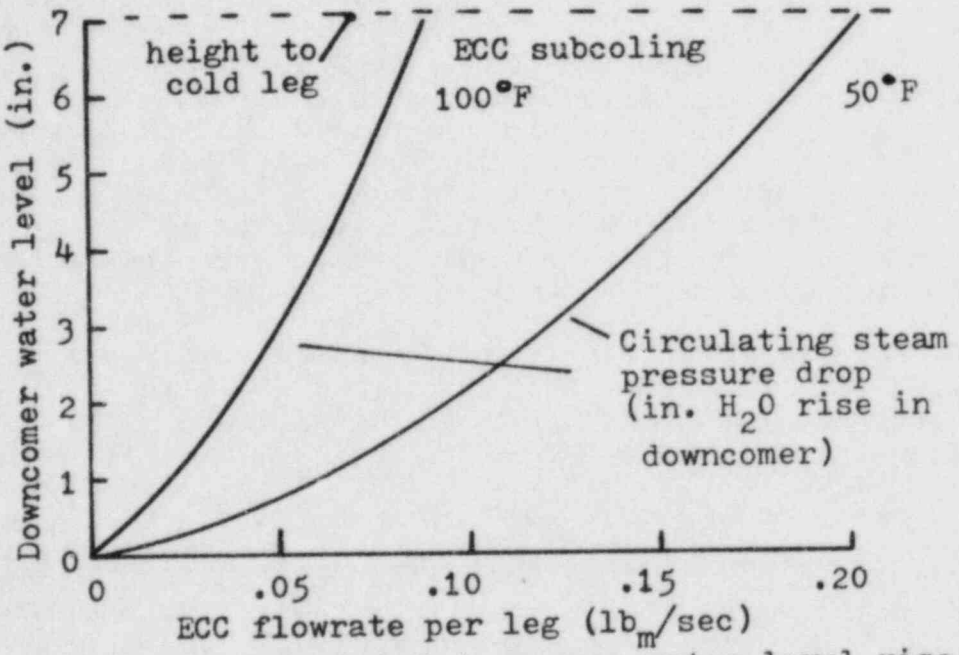

Figure 14 - Calculated downcomer water level rise in experimental model during ECC

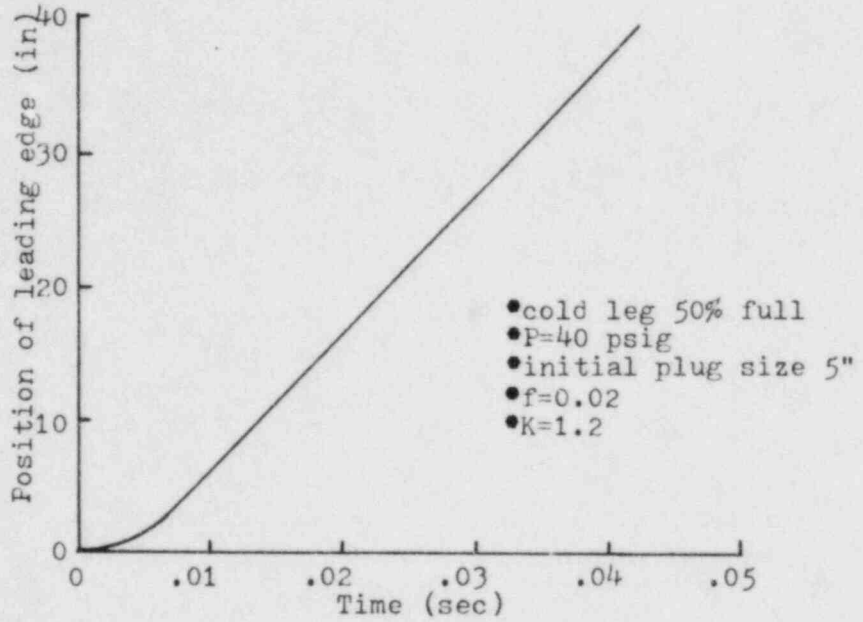

A. Postion of plug

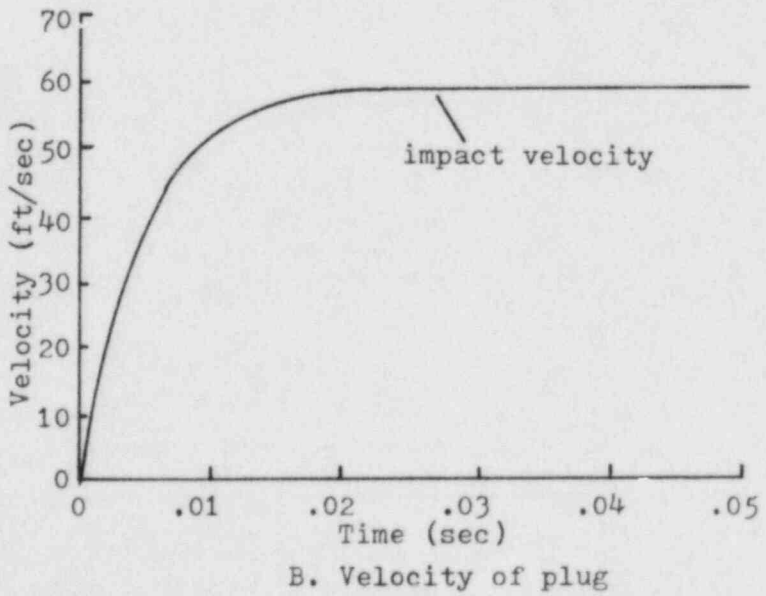

B. Velocity of plug

Figure 15 - Dynamics of liquid plug during steam bubble collapse water hammer in experimental flow model

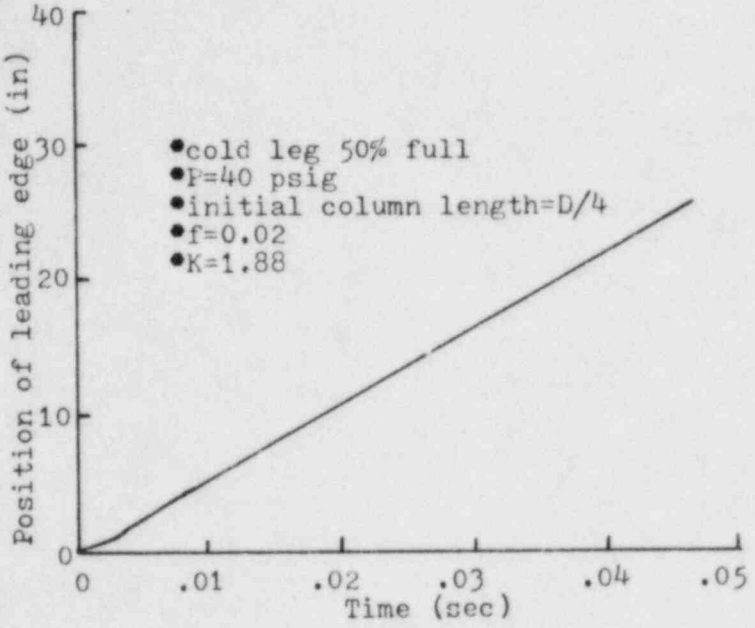

A. Position of water column

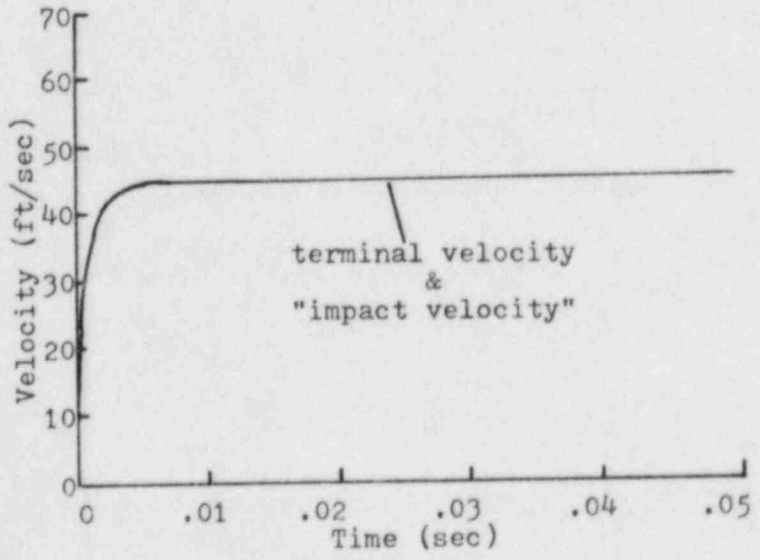

B. Velocity of water column

Figure 16 - Dynamics of water column from core vessel during steam bubble collapse water hammer in experimental flow model

velocities.

The impact pressure is calculated by Eq. 3-20, assuming a speed of sound in an elastic pipe of 3900 ft/sec. Similar calculations were made for other pressures and then water hammer pressure rise was plotted as a function of the experimental model operating pressure and compared to the highest pressure measurements taken. See Figure 17. The highest measured pressure spike 29% of the calculated pressure (@ 30 psig) for the case of the liquid plug hitting the moving column of water from the downcomer. The greatest pressure measured even falls short by about 50% of the potential ressure rise possible neglecting the velocity of the water column from the downcomer, as shown in Figure 17.

The fact that the measured pressure spike is less than the calculated value is not surprising since many factors may contribute to reducing the peak pressure spike measured during water hammer not accounted for in this simple model. It is likely that the pressure transducer was not located at the exact point of plug impact and therefore measurements would be that of a pressure wave attenuated by pipe frictional/momentum losses in traveling from the water plug impact point where it was produced to the pressure transducer. Also the pressure inside the steam bubble only approaches absolute zero depending on the actual rate of steam condensation during bubble collapse. This condensation rate is hampered for instance by the pressure of any non-condensibles in the steam supply (typical air volume fraction of 10^{-4}) or which evolves by dissolution from the liquid below the void during depressurization. The presence of any air bubbles can also substantially diminish the speed of sound in the cold leg from that which was assumed for an elastic pipe (3900 ft/sec). In addition, differences between measurements and calculations can arise due to incorrect accounting for frictional/momentum losses.

5. EVALUATION OF WATER HAMMER IN A PWR DURING ECC INJECTION

5.1 System State

Water hammer is expected to occur during cold leg ECC injection in an actual PWR system that has undergone a SB-LOCA. The state of the system for this to occur must be similar to that model in the flow experiments. The necessary conditions which make water hammer possible and may put the system in jeopardy are as follows:

1. Voided Core
   The core is at least partly voided so that a stratified flow of steam of steam and water exists in the cold legs.

2. Pumps Off
   Reactor coolant pumps are off such that stratified flow conditions are maintained.

3. ECC On
   ECC injection system is engaged to reflood the system.

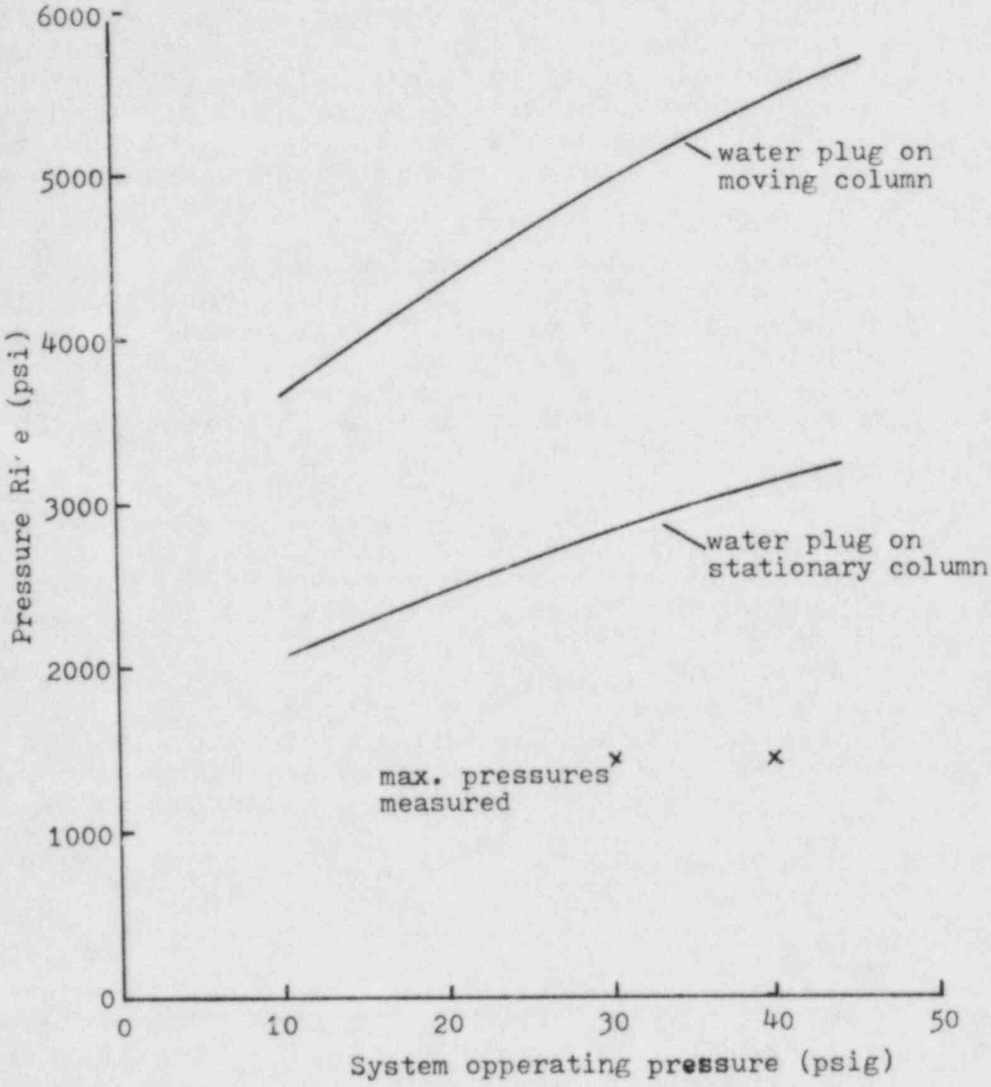

Figure 17 - Comparison of calculated pressure rise during water hammer to measured pressures

Provided that these conditions are met, the system state that can lead to steam bubble collapse water hammer during ECC cold leg injection is depicted in Figure 18 for a B & W plant. The system has undergone a SB-LOCA in which there has been enough coolant loss to cause the cold legs to be voided. The loop seal is plugged because there is no loop circulation. As ECC is being injected into the cold legs, steam which is present in the lines and that which can escape from the inner core vessel through the vent valves, flows toward the points of injection. When the water level and associated steam velocity are such that a liquid plug forms, a volume of steam becomes trapped. As the trapped steam condenses, the water plug in the loop seal and the column of water from the downcomer accelerate into the void. Upon impact, a pressure spike is produced.

5.2 Determination of Stages of Reflood That Can Result In Waterhammer

Water hammer is inevitable for gas free steam during ECC when the cold leg liquid depth becomes sufficiently high enough such that a slug forms, trapping a steam bubble as demonstrated in the flow model tests. The water level in the cold leg depends upon the flow rate of ECC and the water level in the core vessel downcomer which can impede the "free overfall" of coolant into the core. When the ECC flow rate alone is great enough to produce liquid depths for which water hammer is possible and depending on the initial core voidage, numerous water hammers will occur until the core and cold legs are refilled. A smaller number of water hammers will occur at lower ECC flow rates when the cold leg liquid depth increases during refill. One severe water hammer blow itself may produce immediate dynamic loads which can lead to ductile failure of ECC piping, pipe supports, or even the cold leg. However, the greater the number of water hammers, the greater the chance that such piping will fail at lower water hammer pressures due to exceeding material fatigue limitations from successive water hammers.

The absolute stability limit for a typical PWR 28 inch ID cold leg was calculated to determine if the actual HPSI flow rate of a typical plant is great enough to produce the critical liquid depths and steam velocity for water hammer initiation. Figure 19 shows the absolute stability limit as a function of system pressure.

For a constant ECC temperature, this analysis shows that as the operating pressure is increased, the critical flow rate necessary to initiate water hammer decreases primarily because of the greater amount of subcooling (for fixed ECC Temperature) at higher system pressures. This trend can be explained as follows. For a given ECC flow rate, as the system pressure (and saturation temperature) increases, the mass flow rate of steam increases proportionally to the amount of ECC subcooling. A greater steam mass flow rate increases the total flow rate at the overfall ($m_s + m_c$) increasing the critical depth and thus the liquid depth in the cold leg. The increase in steam flow rate combined with a higher liquid depth increases the value of the Taitel-Dukler parameter more than the density change of steam decreases its value. The net effect is that it takes a lower ECC flow rate to produce a value of N_{TD} equal to 1. This is not necessarily a universal truth, but it depends on the system too.

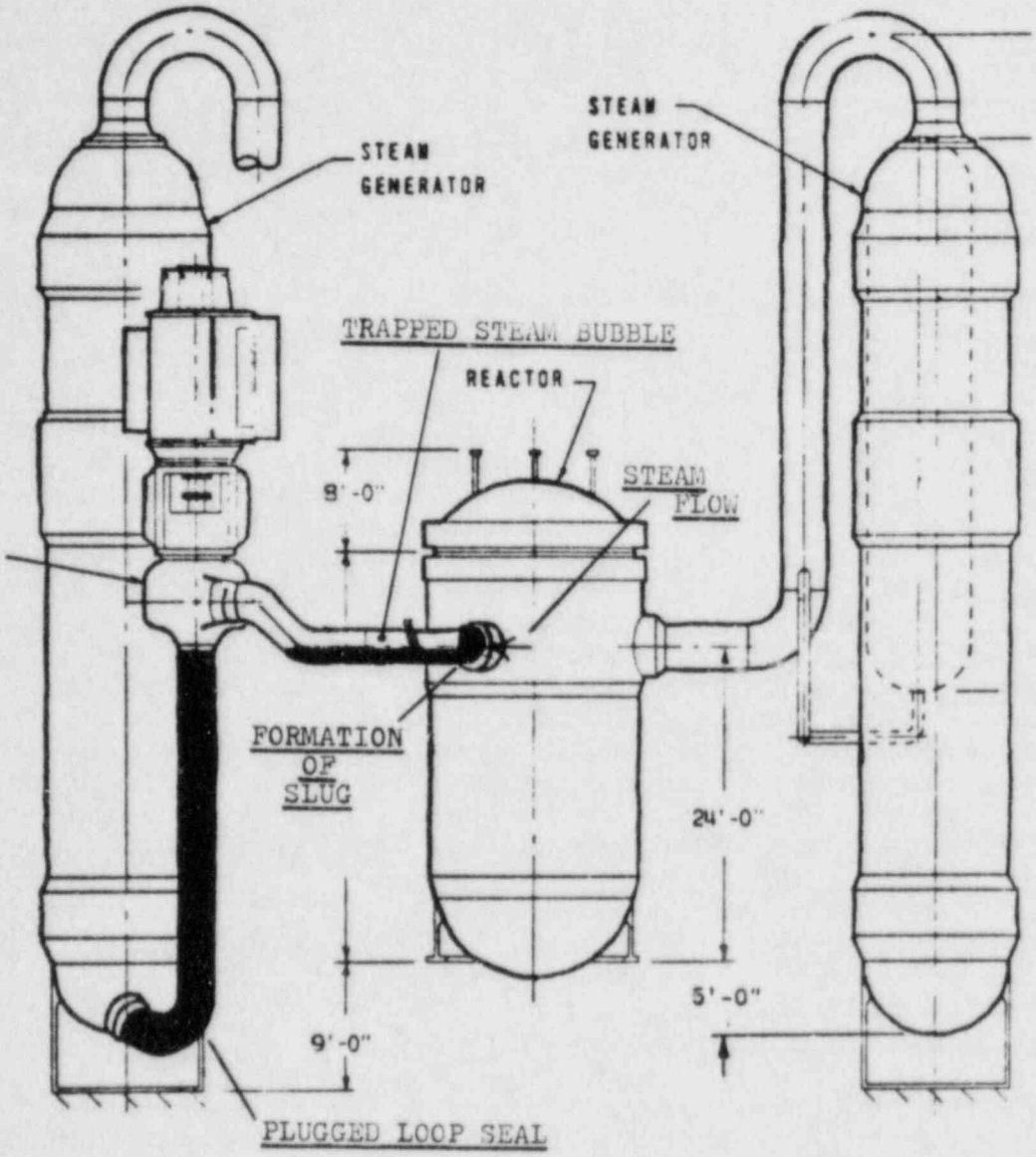

Figure 18 - Postulated steam bubble collapse water hammer during ECC in a PWR (B&W plant shown)

In this figure a comparision of the absolute stability limit is made to the HPSI flow rate of a typical plant, Millstone 3 (from Figure 20). Millstone 3 is a 4 loop, 4 steam generator Westinghouse unit that has 3 charging pumps and 2 safety injection pumps that can be active during HPSI. As shown, the maximum flow rate (run of flow) of the 5 pumps is less than needed to initiate water hammer as calculated by the absolute stability. At high pressures, the pump output is less than the runout flow and absolute stability limit which was approximated as shown in Figure 19.

The absolute stability limit is also greater than the runout flow rate from the high pressure injection system HPIS of a CE plant. The CE-80 reactor system has 4 HPIS pumps with 2 considered operable at any one time. Even if 4 are on, the run out flow rate is 65 lbm/sec per leg which is less than the absolute stability limit (9).

The water depth needed to initiate water hammer, assuming the injection flow rate as a function of system pressure as approximated in Figure 19 and a proportional flow rate of steam necessary to achieve thermal equilibrium was calculated. Figure 21 shows the result of this calculation as a plot of the percentage of flow area occupied by the liquid vs. system pressure. It is expected that for these water levels during refill water hammer can first occur.

In summary, the analysis shows that the HPSI system coolant flow rate is not great enough to cause a cold leg water hammer when there is a free overfall of coolant into the core vessel. However, during refill, water hammers are inevitable although they may be fewer in number. The first occurance of water hammer can be when the water level is as low as that given by Figure 21.

5.3 Calculation of Peak Pressure Rise During PWR Water Hammer

The potential water hammer pressures as a result of steam bubble collapse water hammer during ECC reflood were calculated for a typical reactor coolant system following the methodology described in Section III. The configuration choosen for this study was a CE-80 reactor coolant system which has a loop seal of approximately 27 ft in length (See Figure 22). The differential equations describing the motion of the liquid plugs from the downcomer and loop seal during steam bubble collapse were solved for a variety of system operating pressures.

Figure 23 summarizes the appropriate frictional/momentum loss coefficients for the full scale geometry. The loss coefficient for flow through the reactor coolant pump, approximately 10 velocity heads, is for a pump with a locked rotor. Although the pressure drop actually decreases as the rotor is spinning up, the time it takes for this to happen is much greater than the time duration of the steam bubble collapse so that a constant pressure drop approximation is adequate. For simplicity, it was assumed that the pipe was half full of water upon steam bubble collapse which is approximately correct over a good range of operating pressures as indicated in Figure 21. A typical calculation of the leading edge position and velocity of each plug are plotted as a function of time for 1500 psig operation as shown in Figures 24 and 25.

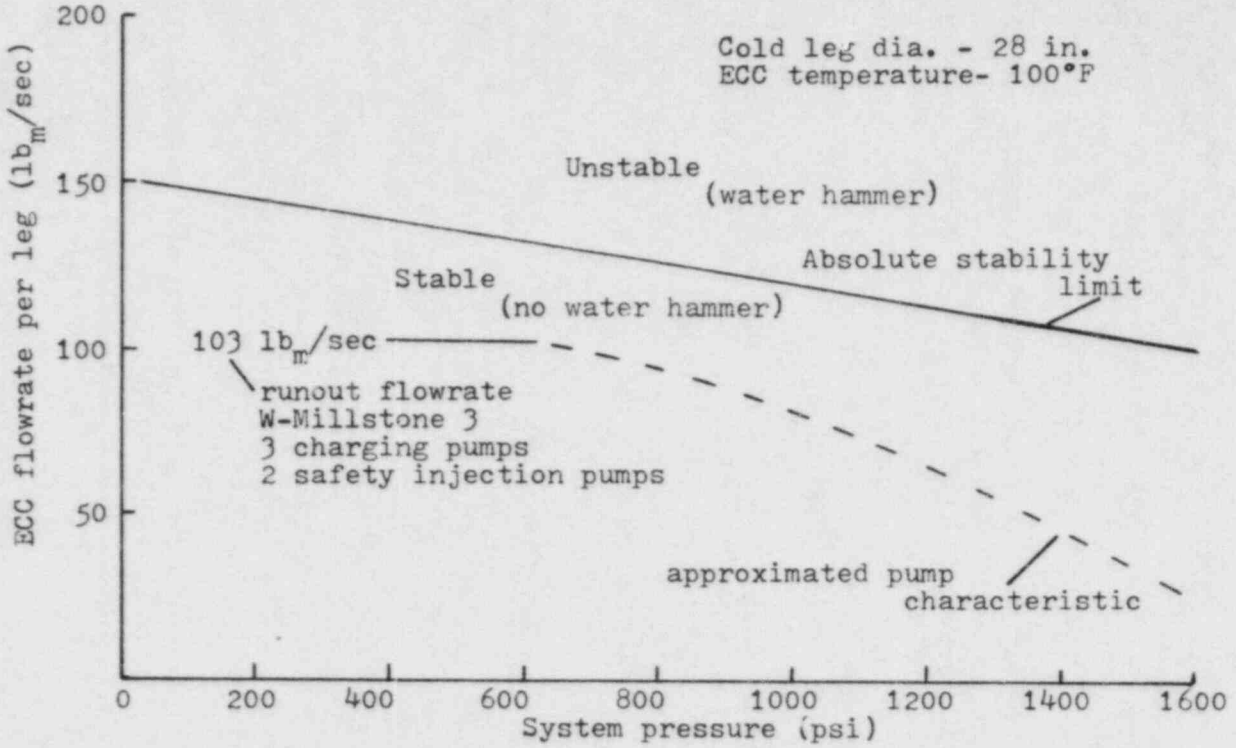

Figure 19 - Comparison of the critical ECC flow rate necessary to cause water hammer during ECC in a typical plant vs. the HPSI system coolant flow output of a W plant

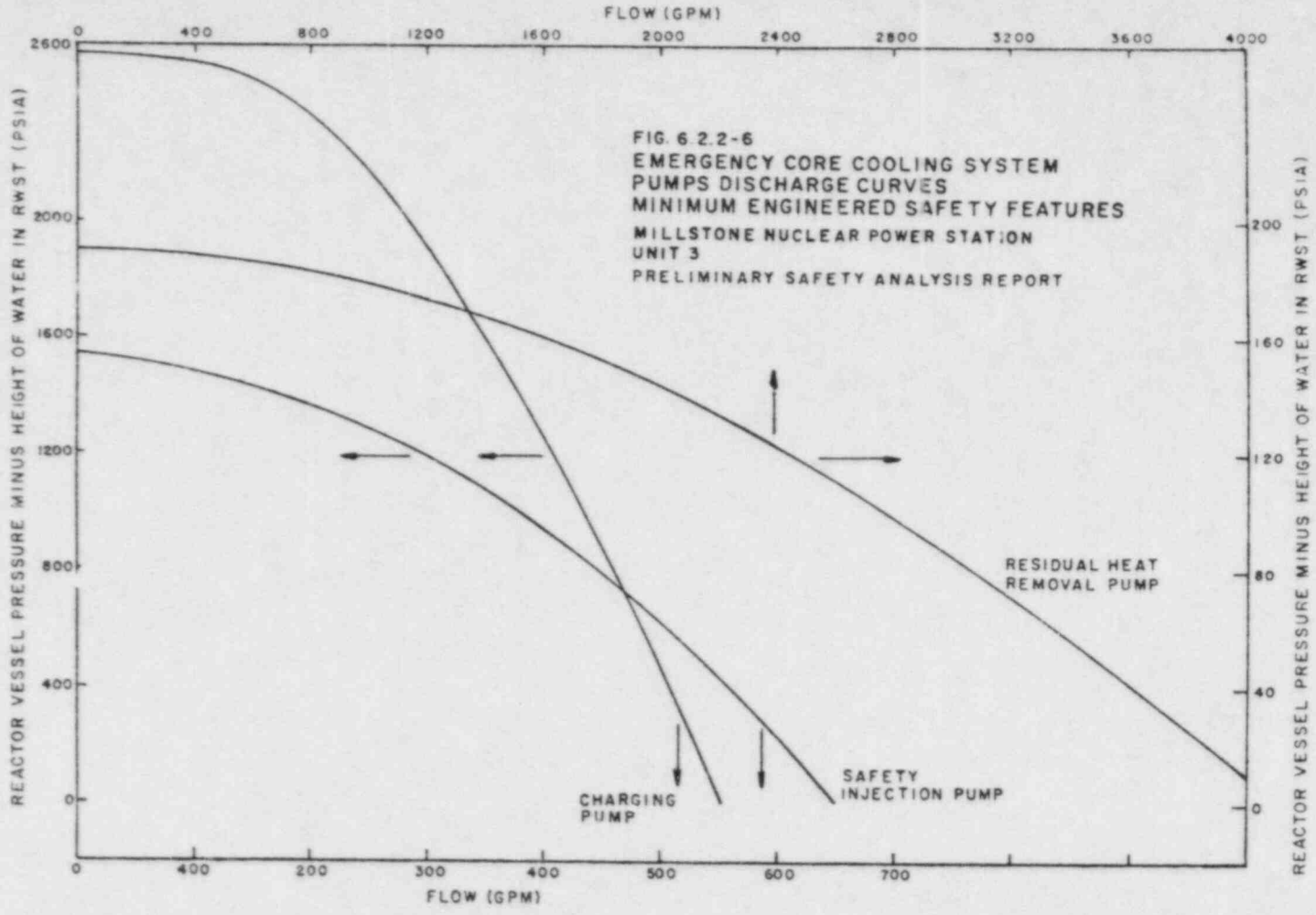

Figure 20 - HPSI flow rate output of a W plant (Ref.8)

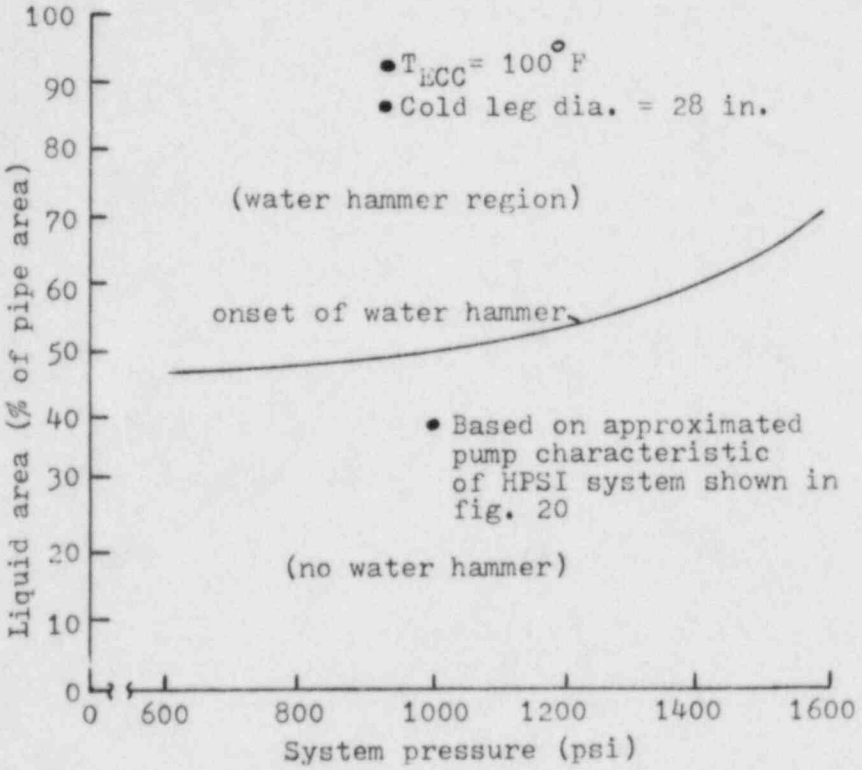

Figure 21 - Approximate cold leg water depths during ECC reflood for which water hammer is predicted in a PWR

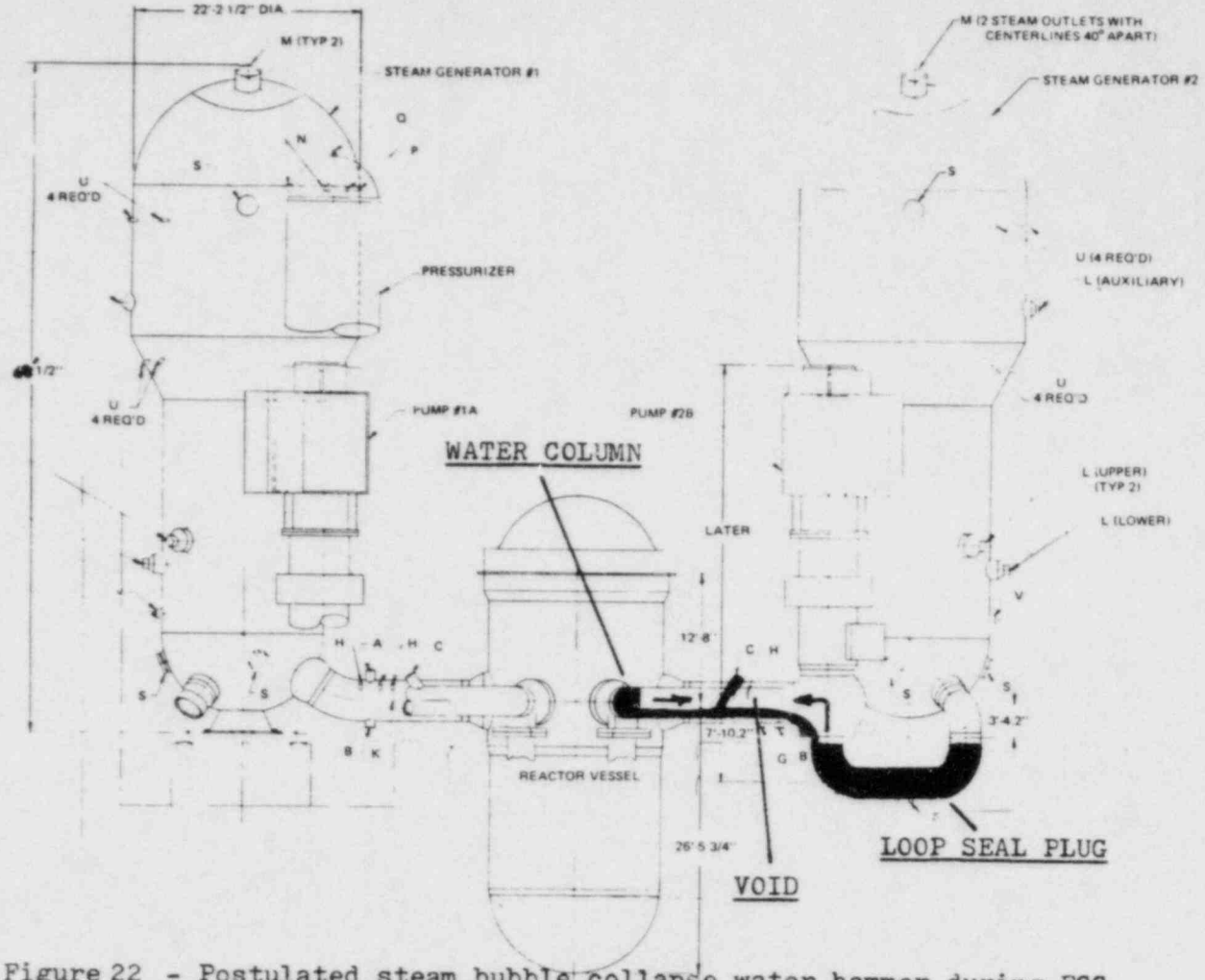

Figure 22 - Postulated steam bubble collapse water hammer during ECC in a CE-80 system used to calculate the resulting pressures

Pressure loss coefficients

Water column from downcomer	$\Delta P/q$
• 90° mitre turn into cold leg	1.20
• entrance loss	0.38
• 45° turn in cold leg	0.30
	K_t = 1.88

Water plug from loop seal	$\Delta P/q$
• 90° bends in loop seal	0.8
• Pump (locked rotor, 0 rpm - see below)	10.2
	K_t = 11.0

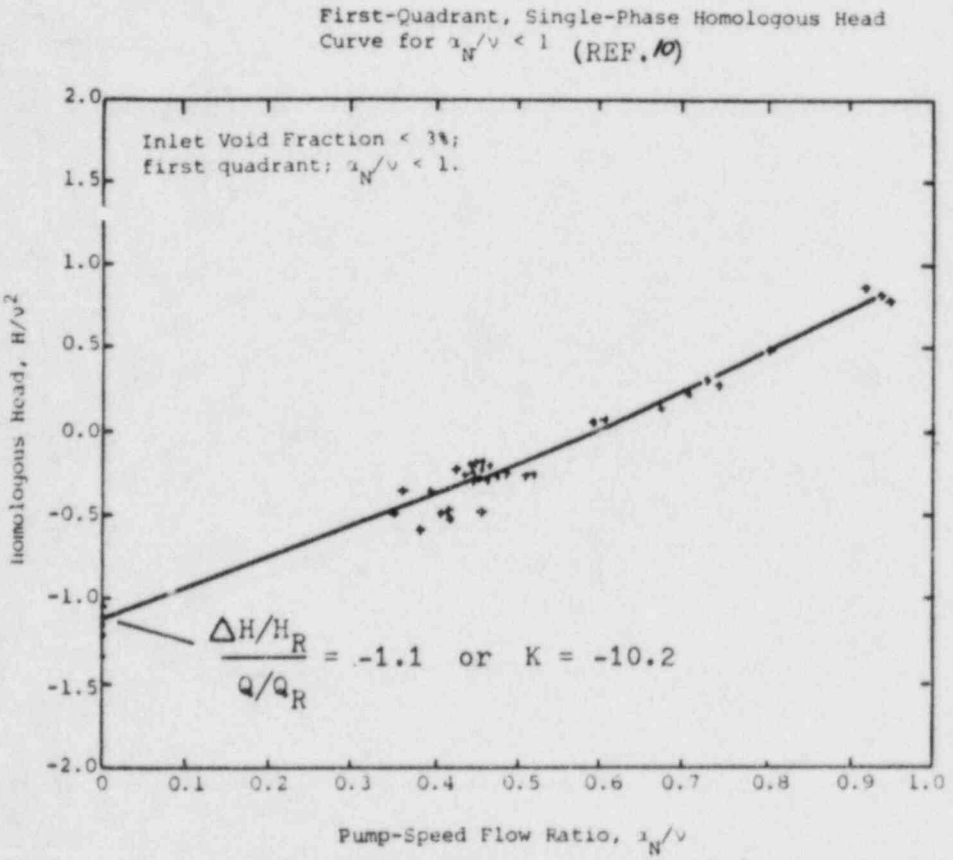

Figure 23 - Summary of pressure loss coefficients of a full scale PWR

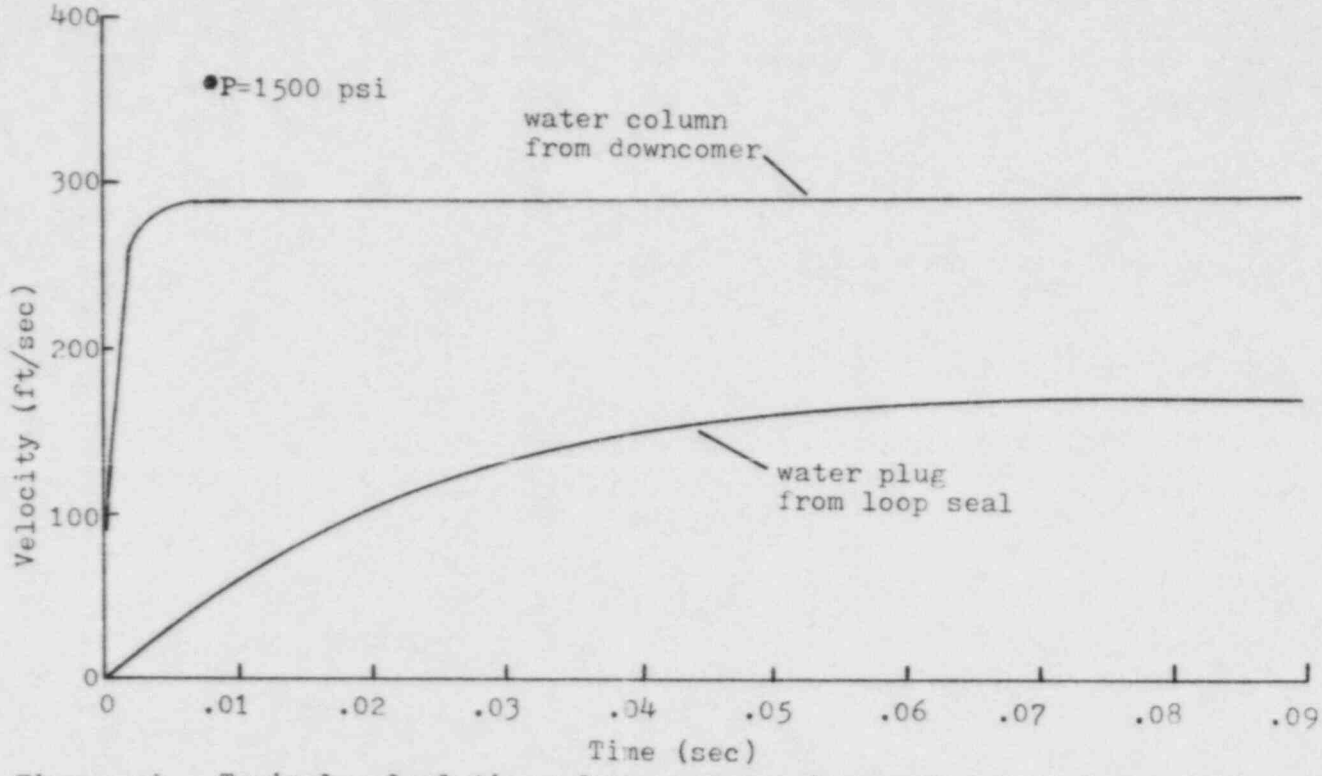

Figure 24 - Typical calculation of the water column and water plug velocities during steam bubble collapse water hammer in a PWR

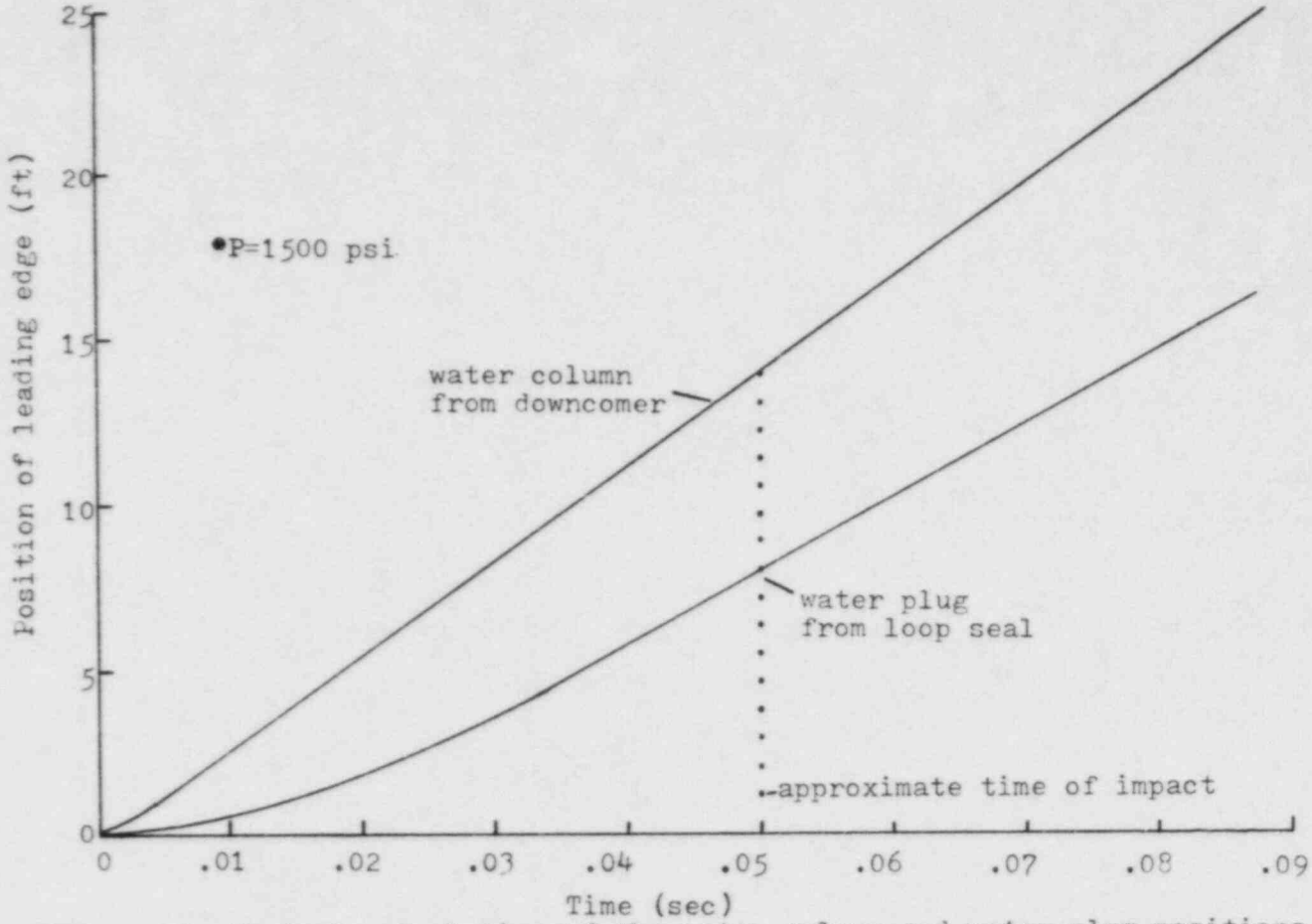

Figure 25 - Typical calculation of the water column and water plug positions during steam bubble collapse water hammer in a PWR

The trapped steam bubble was assumed to extend from the reactor vessel to the reactor coolant pump (approximately 22 ft). Similar to calculations made in the model geometry, impact was assumed when the sum of the distance traveled by both plugs equals this amount.

The core liquid plug transient as calculated is very short in duration because the assumed initial plug length is very small and therefore at impact, the plug has reached its maximum or terminal velocity. Figure 26 shows the effect in choice of initial water column length on the calculated terminal velocity. As shown, the obtainable velocity (and thus potential pressure rise during water hammer) is fairly insensitive to the initial water column length for this case because the obtainable velocity is limited by the various flow resistances and column growth. The effect of the various factors which limit the obtainable velocity of the liquid column are illustrated in Figure 27. As shown, in the ideal case, the velocity of the column approaches that calculated by Bernoulli equation.

Upon impact, the calculated velocity of the loop seal plug is approximately 1/2 of the plug from the core and the resulting pressure spike as calculated increases substantially over what is calculated neglecting the velocity of the plug from the loop seal. Figure 28 gives the potential pressure rise during water hammer as a function of system operating pressure. Even when the velocity of loop seal plug is neglected a substantial pressure rise is predicted due to the impact of the water column on the plug of liquid from the loop seal. For this case, the impulse will act over 11 milliseconds, the time for a wave to the length of the cold leg between the pump and core and return.

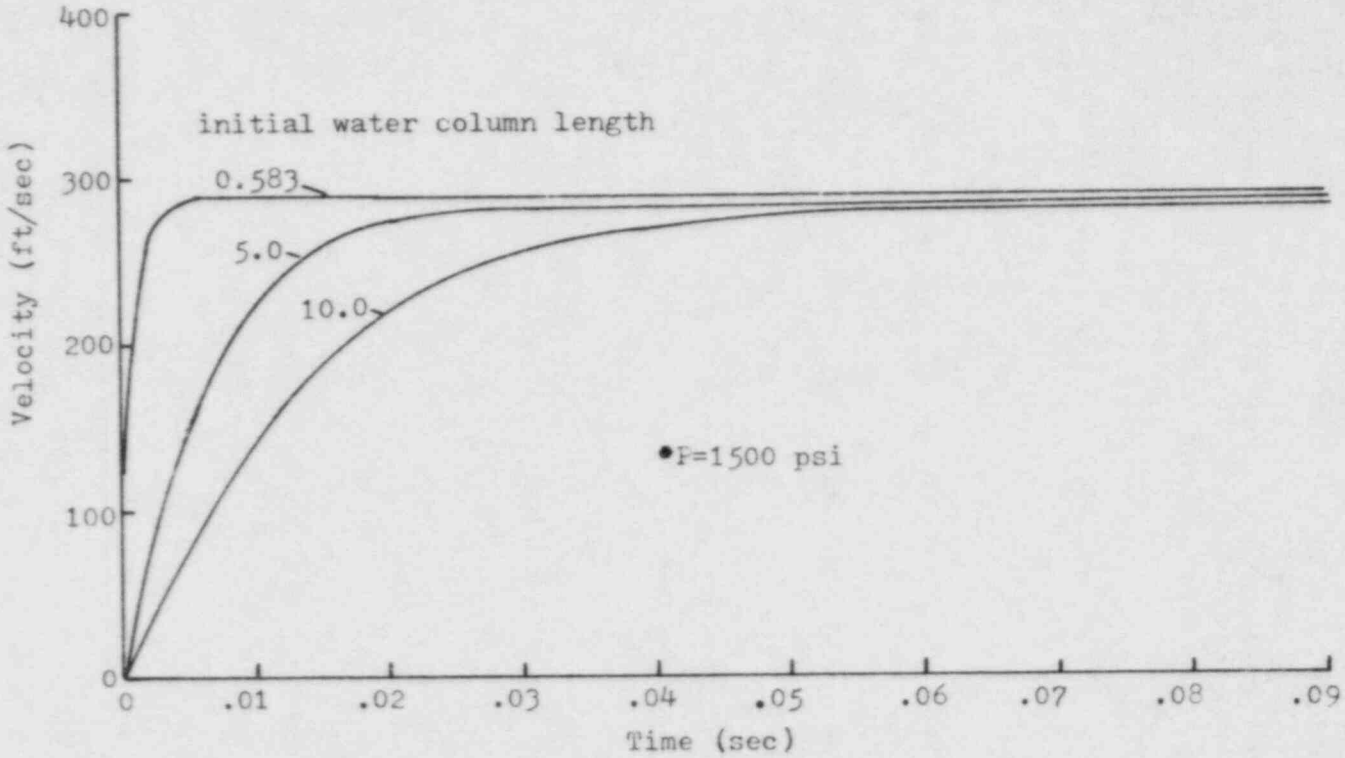

Figure 26 - Dynamics of water column as a function of initial water column length assumed

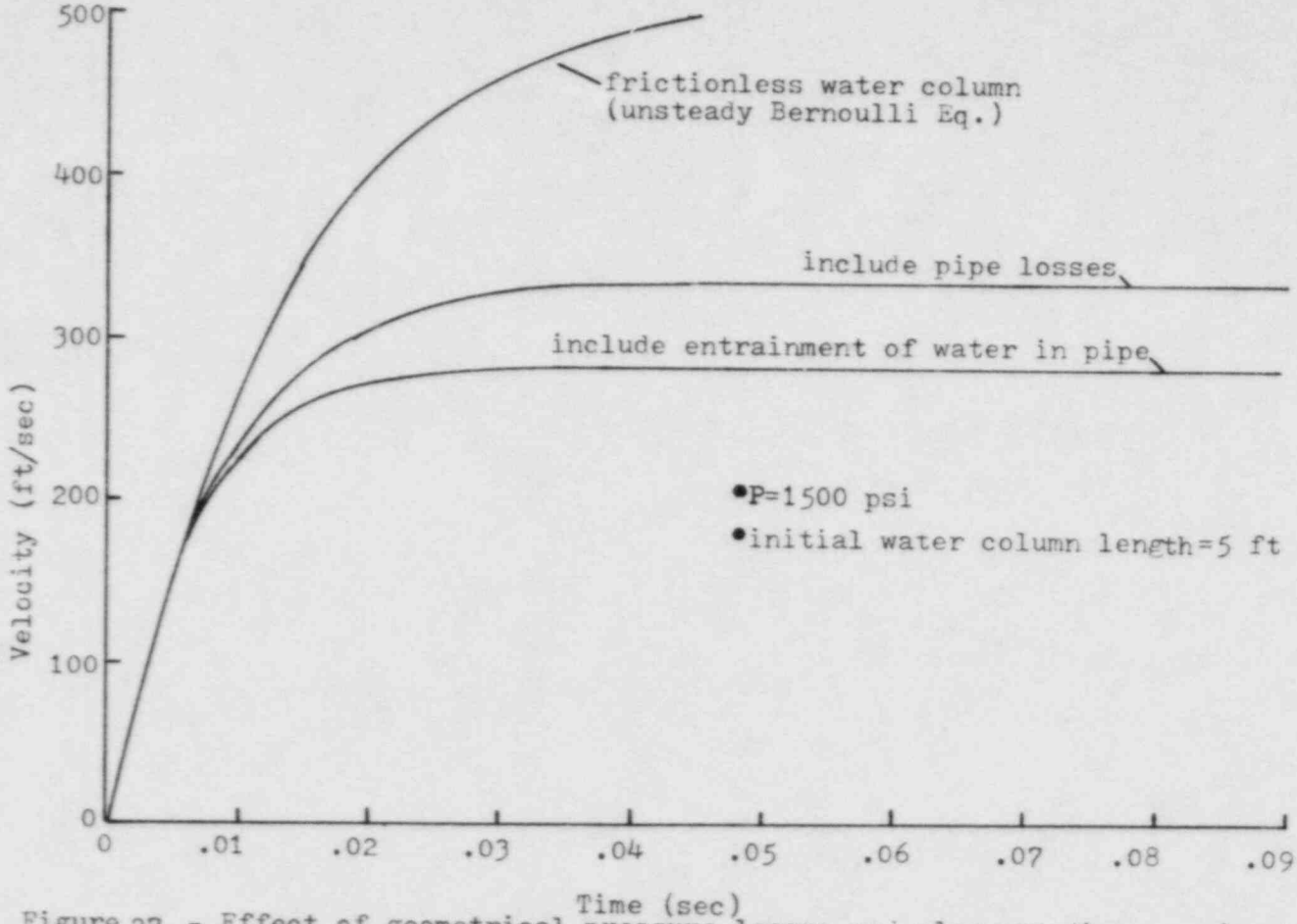

Figure 27 - Effect of geometrical pressure losses and plug growth on maximum obtainable velocity during steam bubble collapse

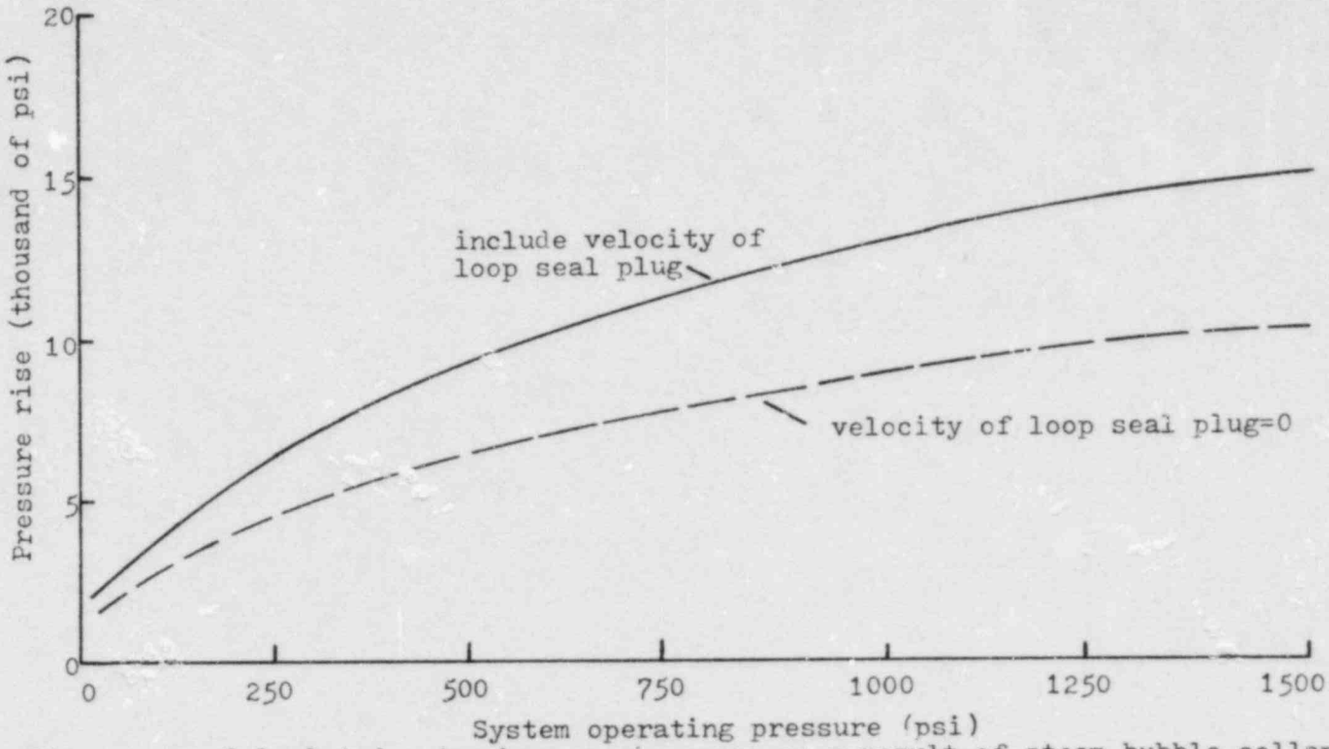

Figure 28 - Calculated water hammer pressures as a result of steam bubble collapse water hammer during ECC in a PWR

6 CONCLUSIONS

1. Simulation of ECC in the experimental flow model has demonstrated steam bubble collapse water hammer when the cold leg water depth became great enough to result in a flow transition from stratified to slug flow.

2. In an actual PWR, the ECC flow rate injected by the HPSI system produces cold leg water depths which are too low to produce "Bjorge type" water hammer.

3. However, water hammer in each cold leg is inevitable when the downcomer fills up to produce the necessary cold leg liquid depths to result in a transition to slug flow. During this stage of reflood, only a small number of such water hammers can even occur.

4. A system having undergone a SB-LOCA characterized by high system operating pressures and gas free steam has the greatest potential for damage during such water hammer.

5. The greatest peak pressures measured in the flow model, which were near the point of ECC injection, were 1/2 of what is calculated assuming the incoming water column from the core downcomer has negligible velocity.

6. Measurement limitations as discussed in this report, and factors such as the presence of non-condensibles, can account for the discrepancy between peak pressure measurements and calculations as well as the conservatism of the calculaton.

7. In an actual PWR the precise details of the location and magnitude of the resulting pressures are truely unpredictable. However, bounding estimates can be made. The calculation scheme used in this report, though a simplification of the actual phenomenon, provides an upper bound valve of the peak pressures possible as a result of such water hammer.

REFERENCES

1. "Water Hammer in Nuclear Power Plants," NUREG-0582, Division of Systems Safety, July, 1979.

2. Bjorge, Robert W., "Initiation of Water Hammer in Horizontal and Nearly Horizontal Pipes Containing Steam and Sub-cooled Water," Ph.D. thesis, Massachusetts Institute of Technology, 1982.

3. Elliott, J.L., Lime, J.F., Wilcutt, G.J.E., "Effect of Pump Operation Following a Small Break in a Pressurized Water Reactor," Proceedings of the International Meeting on Thermal Nuclear Reactor Safety, NUREG/CP-0027, p. 867.

4. Taitel, Yehuda, and Dukler, A.E., "A Model for Predicting Flow Regime Transitions in Horizontal and Near Horizontal Gas-Liquid Flow," AlChE Journal, 22, 1976, pp. 47-55.

5. Chow, Ven Te, Open Channel Hydraulics, McGraw-Hill, New York, 1959, p. 82.

6. Braine, C.D.C., "Draw-Down and Other Factors Relating To The Design of Storm-Water Outflows on Sewers," Journal, Institution of Civil Engineers, London, Vol. 25, No. 6, 1947, pp. 136-163.

7. Gruel, R.L. Huber, P.W. and Hurwitz, W.M., "Piping Response to Steam-Generated Water Hammer," ASME J. Pressure Vessel Technology, 103, p. 219.

8. Millstone Nuclear Power Station Unit 3, Preliminary Safety Analysis Report, 1972.

9. Anderson et al, "Loft Typicality Evaluation," Combustion Engineering Inc., Vol. 1, 1973, p. 38.

10. Winks, R.W., Parks, C.E., "One-Third-Scale Air Water Pump Programs Test Program and Pump Performance," EPRI NP-135, 1977, pp. 6-17.

NRC FORM 335 (7.77) U.S. NUCLEAR REGULATORY COMMISSION

BIBLIOGRAPHIC DATA SHEET

1. REPORT NUMBER *(Assigned by DDC)*: NUREG/CR-3895

4. TITLE AND SUBTITLE *(Add Volume No., if appropriate)*: INVESTIGATION OF COLD LEG WATER HAMMER IN A PWR DU. TO THE ADMISSION OF ECC DURING A SMALL BREAK LOCA

2. *(Leave blank)*

3. RECIPIENT'S ACCESSION NO.

7. AUTHOR(S): A.B. Jackobek and P. Griffith

5. DATE REPORT COMPLETED: MONTH January YEAR 1984

9. PERFORMING ORGANIZATION NAME AND MAILING ADDRESS *(Include Zip Code)*:
Massachusetts Institute of Technology
Department of Mechanical Engineering
Cambridge, MA 02139

DATE REPORT ISSUED: MONTH September YEAR 1984

6. *(Leave blank)*

8. *(Leave blank)*

12. SPONSORING ORGANIZATION NAME AND MAILING ADDRESS *(Include Zip Code)*:
Division of Accident Evaluation
Office of Nuclear Regulatory Research
United States Nuclear Regulatory Commission
Washington, D.C. 20555

10. PROJECT/TASK/WORK UNIT NO.

11. CONTRACT NO: B7229

13. TYPE OF REPORT: Technical

PERIOD COVERED *(Inclusive dates)*

15. SUPPLEMENTARY NOTES

14. *(Leave blank)*

16. ABSTRACT *(200 words or less)*

Experimental studies using a protoypical flow model of a pressurized water reactor (PWR) demonstrate water hammer in the cold legs due to the admission of emergency core cooling (ECC). Such water hammer can occur in an actual PWR during reflood provided there exists a stratified flow of steam and water in the cold legs. The hydraulic are postulated in this report. Calculations, based on a published criterion for water hammer initiation, show that the amount of ECC administered by the high pressure safety injection (HPSI) system, is not great enough to produce liquid depths in the cold leg which can lead to slug formation and subsequent steam bubble collapse water hammer. However, a few water hammers can occur during ECC as the cold leg is being refilled.

A simple analysis developed in this report calculates the water hammer pressures possible under these postulated flow conditions. Potentially dangerous water hammer pressures are predicted during reflood at high system operating pressures characteristic of a small break loss-of-coolant accident (SB-LOCA). Similiar calculations done for the geometry of the experimental apparatus were compared to measurements taken during water hammer.

17. KEY WORDS AND DOCUMENT ANALYSIS

17a. DESCRIPTORS

PWRS (Pressurized Water Reactors Water Hammer)
Emergency Core Cooling
Small Break Loss-of-Coolant Accident (SB-LOCA)
High Pressure Safety Injection System (HPSI)

17b. IDENTIFIERS/OPEN-ENDED TERMS

18. AVAILABILITY STATEMENT: Unlimited

19. SECURITY CLASS *(This report)*: Unclassified

21. NO. OF PAGES

20. SECURITY CLASS *(This page)*

22. PRICE: $

NUREG/CR-3895

INVESTIGATION OF COLD LEG WATER HAMMER IN A PWR DUE TO THE ADMISSION OF EMERGENCY CORE COOLING (ECC) DURING A SMALL BREAK LOCA

SEPTEMBER 1984